A New Class of Endoplasmic Reticulum Export Signal ΦXΦXΦ for Transmembrane Proteins and its Selective Interaction with Sec24C

（膜蛋白質小胞体輸出の分子機構：新規シグナル配列ΦXΦXΦと Sec24C の選択的相互作用）

Wataru Otsu

Contents

Abbreviations

The abbreviations used in this study are as follows:

AE1 ..... anion exchanger 1

AE1Δ11 ..... erythroid AE1 lacking the 11 C-terminal amino acid residues

bAE1 ..... bovine AE1

COPII ..... coatomer protein complex II

EGFP ..... enhanced green fluorescent protein

endo H ..... endoglycosidase H

ER ..... endoplasmic reticulum

FT-MS/MS ..... Fourier transform-tandem mass spectrometry

hAE1 ..... human AE1

kAE1 ..... kidney AE1

PBS ..... phosphate-buffered saline

SDS-PAGE ..... sodium dodecyl sulfate polyacrylamide gel electrophoresis

VSV-G ..... vesicular stomatitis virus glycoprotein

In the present study, one-letter and three-letter abbreviations for amino acid residues are employed.

Preface

Export from the endoplasmic reticulum (ER) is the first sorting event in the vesicular trafficking of membrane proteins to their final destinations in the cell. It is a selective process and is mediated through coatomer protein complex II (COPII)-coated transport vesicles that are formed from three principal components, Sar1-GTP, Sec23/Sec24, and Sec13/Sec31 protein complexes. A number of recent studies have demonstrated that the recruitment of cargo to COPII vesicles is mediated by ER export motifs on the cytoplasmic regions of the cargo. Sec24 acts as the primary cargo selection element of the coat. The presence of multiple Sec24 isoforms (Sec24A–Sec24D), with at least four cargo binding sites on each isoform, and various ER export signals to which Sec24 can bind appears to regulate diverse range and specificity of cargo-Sec24 interactions. However, information on ER export signal motifs are limited to date, although several motifs including di-acidic and di-hydrophobic sequences and their interactions with Sec24 molecules have been characterized extensively.

Anion exchanger 1 (AE1, also known as band 3 in red cells) is critical for the mechanical stabilization of the red cell membrane and in maintaining the acid-base homeostasis. Various mutations of the AE1 gene in humans and animals cause hereditary spherocytosis and distal tubular acidosis. Some of these diseases are caused by targeting defect due to impairment of the AE1-transport vesicle interaction. The previous studies of our group on the mechanisms underlying the ER quality control of the AE1 mutant in cattle have suggested that AE1 has distinct signals for ER exit in different cell types and/or that AE1

proteins from different species use distinct codes for ER export. However, the mechanism responsible for ER export, including the selectivity of AE1 for the COPII machinery, remains unknown.

The purpose of the present study was to examine the signal motif responsible for the ER export and efficient plasma membrane expression of bovine erythroid AE1. The present study shows the intracellular transport of a series of AE1 mutants and chimeric proteins of AE1 and Ly49E, a type II transmembrane protein, and demonstrates the ΦXΦXΦ sequence as a new class of ER export motif and this motif exclusively interacts with Sec24C to facilitate ER-Golgi transport.

The present study has been published as described below.

Otsu, W., Kurooka, T., Otsuka, Y., Sato, K., and Inaba, M. (2013) A new class of endoplasmic reticulum export signal ΦXΦXΦ for transmembrane proteins and its selective interaction with Sec24C. *J. Biol. Chem.* **288**, 18521-18532.

Introduction

Export from the endoplasmic reticulum (ER) is the first sorting event in the vesicular transport of membrane proteins to their final destinations in the cell. In general, selective export from the ER depends on the interaction between an export signal motif in the cytoplasmic regions of the cargo and a cargo-recognition site on the coatomer protein complex II (COPII) coat (Bonifacino and Glick, 2004; Mancias and Goldberg, 2005; Mellman and Nelson, 2008). Several ER export motifs have been identified, and di-acidic (D/E)X(D/E) and di-hydrophobic (FF, LL, VV *etc*.) motifs have been well characterized. Di-acidic motifs have been identified in several stomatitis virus glycoprotein (VSV-G) (Nishimura and Balch, 1997), cystic fibrosis transmembrane-conductance regulator (CFTR) (Wang *et al*., 2004) and some inwardly rectifying potassium channels (Ma *et al*., 2001). Di-hydrophobic motifs are required for the ER export of ERGIC53 (Nufer *et al*., 2002; Nufer *et al*., 2003). Moreover, the LXXLE motif of the yeast SNARE protein, Bet1 (Miller *et al*., 2003; Mossessova *et al*., 2003), the IXM motif of the SNARE proteins, membrin and syntaxin 5 (Mancias and Goldberg, 2008), and the RI/RL motifs in serotonin and GABA transporters are ER export codes (Farhan *et al*., 2007; Sucic *et al*., 2011).

COPII-coated vesicles comprise three principal components, Sar1-GTP, Sec23/Sec24 and Sec13/Sec31 protein complexes, which function in concert to promote budding of vesicles for transport (Mancias and Goldberg, 2005; Russell and Stagg, 2010; Gillon *et al*., 2012; Zanetti *et al*., 2012). Sec24 is the primary cargo selection element of the coat (Miller *et al*., 2003; Mossessova *et al*., 2003; Bonifacino and Glick, 2004). In mammals, the presence of multiple Sec24 isoforms (Sec24A–Sec24D), with at least four cargo binding sites on each

isoform, means that there are a number of ER export signals to which Sec24 can bind, and that the range and specificity of cargo-Sec24 interactions is diverse (Russell and Stagg, 2010; Gillon *et al*., 2012; Zanetti *et al*., 2012). For example, di-hydrophobic motifs bind to all four Sec24 isoforms with varying strength (Wendeler *et al*., 2007). While the LXXLE and DXE classes of signals selectively bind to Sec24A/Sec24B, the IXM sequence specifically binds to the surface groove on Sec24C/Sec24D, which is occluded in Sec24A/Sec24B (Mancias and Goldberg, 2008). Furthermore, there are several examples in which a single isoform is absolutely required; for example, Sec24C and Sec24D differentially mediate the ER export of the highly related neurotransmitter transporters of serotonin and GABA (Farhan *et al*., 2007; Sucic *et al*., 2011). No human diseases resulting from genetic defects in Sec24 have been found to date; however, animal models of defects in some Sec24 isoforms, human diseases due to the defects in other components of the COPII pathway (Khoriaty *et al*., 2012), and a subtype of cystic fibrosis due to a missense mutation of CFTR at the di-acidic ER export signal (Tzetis *et al*., 2001; Wang *et al*., 2004) have been reported. It is conceivable that impairment of the cargo-Sec24 interaction can affect ER-Golgi transport and subsequent expression of membrane proteins in the appropriate compartments of the cell, thereby causing various disease phenotypes.

Anion exchanger 1 (AE1, also known as band 3) is expressed primarily in the plasma membrane of red blood cells and the intercalated cells of the renal collecting duct. AE1 is critical for the mechanical stabilization of the red cell membrane by linking the membrane skeleton to the lipid bilayer through association with the anchor protein ankyrin, and in maintaining the acid-base balance through rapid Cl^-/HCO_3^- exchange across the membrane (Tanner, 2002; Alper, 2006). AE1 proteins in the kidney and red blood cells have different N-terminal structures. Human erythroid AE1 possesses an N-terminal stretch consisting of 65

amino acid residues (Fig. 1). Various mutations of the AE1 gene (*SLC4A1*) in humans and animals cause hereditary spherocytosis and distal renal tubular acidosis, which are dominantly inherited (Inaba *et al*., 1996; Yenchitsomanus *et al*., 2005; Alper, 2006). Human kidney AE1 (kAE1) with a nonsense mutation at Arg^{901}, which truncates AE1 by 11 amino acid residues at the C-terminus (kAE1Δ11), impairs the basolateral sorting of the protein in polarized epithelial cell lines. The conserved tyrosine-based YXXΦ motif (X is any amino acid and Φ is a hydrophobic amino acid), which corresponds to ^{904}YDEV^{907} in human erythroid AE1, is involved in the membrane trafficking of kAE1 to the basolateral membrane (Devonald *et al*., 2003; Toye *et al*., 2004) along with a tyrosine residue in the N-terminal cytoplasmic domain (Williamson *et al*., 2008). Interestingly, kAE1Δ11 is retained in the ER in non-polarized Madin-Darby canine kidney cells (Toye *et al*., 2002; Toye *et al*., 2004) and HEK293 cells (Quilty *et al*., 2002). The ^{904}YDEV^{907} sequence is not necessary for the plasma membrane targeting of erythroid AE1, since the AE1 content in red blood cells from patients with the Δ11 mutation is only mildly reduced (Toye *et al*., 2002).

During a series of studies on the mechanism(s) underlying the ER quality control of the AE1 mutant (Inaba *et al*., 1996; Ito *et al*., 2006), we found that the highly conserved C-terminal ELXXL(D/E) sequence, which conforms to the LXXLE class motif, is essential for efficient expression of AE1 at the plasma membrane in transfected HEK293 cells (Adachi *et al*., 2009). We also showed that bovine and murine erythroid AE1 lacking the C-terminal Y XXΦ motif (AE1Δ11) are successfully transported to the plasma membrane, whereas human erythroid AE1Δ11 is retained in the ER (Quilty *et al*., 2002). These findings suggest that AE1 in non-polarized cells (erythroid and HEK293) and polarized cells (renal epithelial and polarized MDCK) have different signals for ER exit and/or that AE1 proteins from different

species use distinct codes for ER export. However, the mechanism responsible for ER export, including the selectivity of AE1 for the COPII machinery, remains unknown.

In the present study, we examined the signal motif responsible for the ER export and efficient plasma membrane expression of bovine erythroid AE1 (bAE1). We analyzed the intracellular transport of a series of AE1 mutants and chimeric proteins of AE1 and Ly49E. Ly49E is a type II transmembrane protein that is expressed in natural killer cells of fetal mice and is a member of the Ly49 receptor family, which recognizes MHC class I molecules (Van Beneden *et al*., 2001; Yokoyama and Plougastel, 2003). A hydrophobic cluster resembling a ΦXΦXΦ sequence in the N-terminal stretch of bAE1 significantly increased the ER exit of AE1 and the AE1-Ly49E chimera through the COPII pathway, irrespective of whether the C-terminal YXXΦ motif was absent or present. We demonstrate that the ΦXΦXΦ motif exclusively interacts with Sec24C at the binding site for the IXM motif, which is also present in Sec24D (Mancias and Goldberg, 2008), to facilitate ER-Golgi transport.

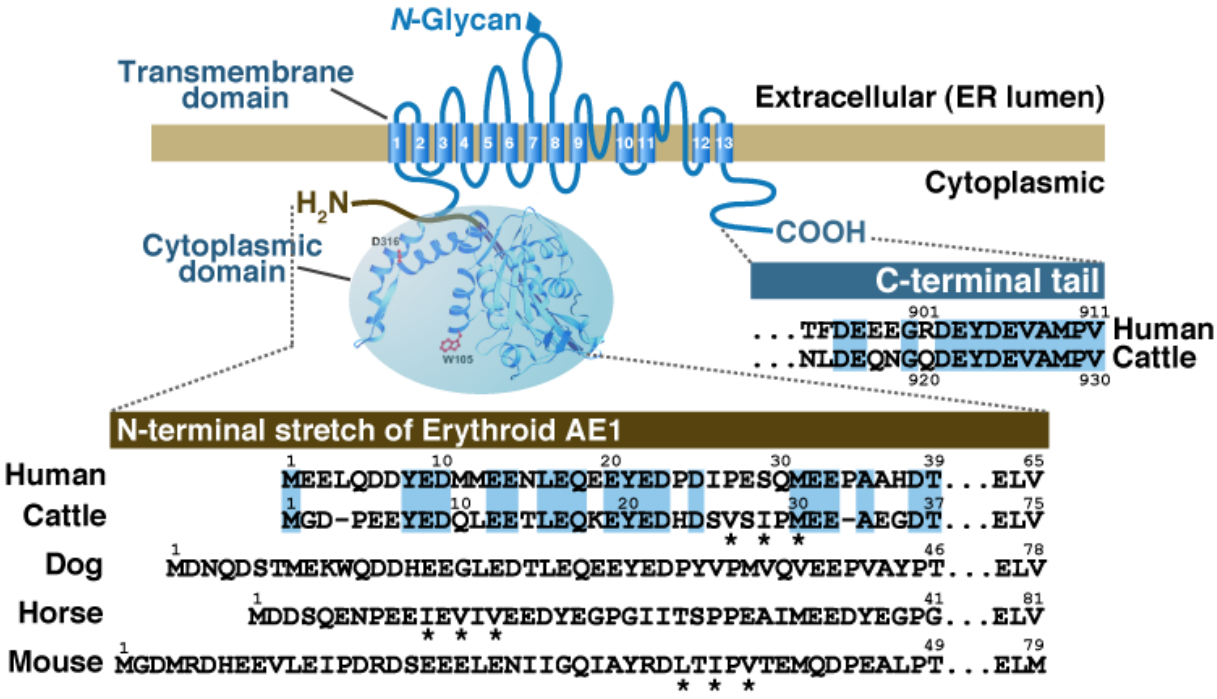

Figure 1. Schematic illustration for erythroid AE1 and the amino acid sequence alignment of N-terminal and C-terminal regions between several species. Schematic illustration of erythroid AE1 based on the crystallographic structure of the cytoplasmic domain (Zhang *et al*., 2000) and the topology model of the transmembrane domain (Zhu *et al*., 2003). The amino acid sequences of the N-terminal and C-terminal regions of human and bovine AE1 are aligned and residues highlighted in blue are identical between human and cattle. The N-terminal sequences of canine, equine, and murine AE1 are also shown. The N-terminal sequence varies between the species. The functions of these amino acid sequences in ER export were analyzed in the present study and asterisks indicate the hydrophobic residues that correspond to the ΦXΦXΦ motif.

Materials and Methods

Antibodies

The antibodies used were: anti-GFP (MBL, Nagoya, Japan), anti-myc (BD Biosciences Clontech), anti-calnexin (Stressgen, Victoria, BC, Canada), anti-GM130 (BD Transduction Laboratories), and anti-Sec23 and anti-ERGIC53 (Sigma-Aldrich).

Construction of plasmids

Plasmid vectors encoding N-terminally enhanced GFP (EGFP)-tagged bAE1 and bAE1Δ11, and mouse erythroid AE1 (pEGFP-bAE1, pEGFP-bAE1Δ11, and pEGFP-mAE1, respectively) were prepared as described previously (Ito *et al*., 2006; Adachi *et al*., 2009). Erythroid AE1 cDNAs for human, dog, and horse (GenBank accession numbers, NM_00342, AB242565, and AB242566, respectively) were obtained by PCR amplification of cDNAs from K562 cells and bone marrow cells from healthy dogs and horses, respectively. The cDNA fragments for AE1 were subcloned into the pEGFP-C3 vector (BD Biosciences Clontech) and the Δ11 truncation mutants were generated by PCR using the appropriate primer pairs as described previously (Adachi *et al*., 2009). The nucleotide sequences of the PCR primers used in the present study are shown in Table 1.

To prepare chimeric AE1 consisting of the bovine N-terminal cytoplasmic domain (amino acid residues 1–403) and the human C-terminal transmembrane domain with or without the Δ11 mutation (designated hAE1Δ11/b[1–403] and hAE1/b[1–403], respectively),

we created the Eco RV site at the position corresponding to ^{403}DI^{404} by PCR without causing any amino acid substitutions. Then, the cytoplasmic domain (residues 1–385) of hAE1 or hAE1Δ11 was replaced by the bovine sequence using the endogenous *Eco* RV site in the hAE1 sequence. Conversely, to make the construct for bAE1/h[1–385] or bAE1Δ11/h[1–385], the cDNA fragment encoding the bovine transmembrane domain was connected to the sequence encoding the cytoplasmic domain of hAE1 (or hAE1Δ11) using the *Eco* RV site. Similar procedures were employed to prepare plasmid vectors for a series of AE1 chimeras, except that the hAE1/b[25-29] and bAE1/h[26-31] vectors and their Δ11 forms were generated by PCR amplification using primers to introduce the appropriate amino acid substitutions (Fig. 3). Likewise, vectors encoding a series of substitution mutants (Fig. 6) were produced by PCR amplification using the appropriate mutagenic primers (Table 1).

cDNA containing the entire coding region of murine Ly49E (GenBank accession number, NM_008463) was obtained by PCR amplification of whole cDNA obtained from a C57BL/6 mouse fetus and was inserted into the pEGFP-N3 vector (BD Biosciences Clontech). The cDNA fragment encoding the N-terminal cytoplasmic region of Ly49E was replaced by the 37 (bovine) or 39 (human) N-terminal amino acid residues of erythroid AE1 (bN[1–37] and hN[1–39], respectively) to create vectors encoding the AE1 N-terminus-Ly49E chimeric protein that was C-terminally tagged with EGFP, namely bN[1–37]Ly, hN[1–39]Ly, and hN[P27V/S29I]Ly.

cDNA for the entire coding region of human Sar1A, Sec24A, Sec24B, Sec24C, and Sec24D (GenBank accession numbers, NM_001142648, NM_021982, NM_006323,

NM_004922, and NM_014822, respectively) were obtained by PCR amplification of HEK293 cell cDNA. Sar1A cDNA was elongated at the 3' end using a primer containing the c-myc epitope peptide (H_2N-QKLISEEDL-COOH) and subcloned into the pcDNA3.1 vector (Invitrogen, San Diego, CA). An activated GTP-bound form of Sar1A, Sar1A H79G (Aridor *et al*., 1995), was generated by site-directed mutagenesis as described previously (Ito *et al*., 2006). The cDNA for each Sec24 isoform was cloned into the pCMV-Myc vector (BD Biosciences Clontech) to generate C-terminally myc-tagged Sec24 proteins. Sec24C-AAA, in which the amino acid residues ^{895}LIL^{897} were mutated to ^{895}AAA^{897} (Mancias and Goldberg, 2008), was generated by site-directed mutagenesis.

cDNA encoding VSV-G was obtained by PCR amplification of the pMD2.G vector (Addgene) and was subcloned into the pEGFP-N3 vector. Primers for these procedures are shown in Table 1.

All experimental procedures met with the approval of the Laboratory Animal Experimentation Committee, Graduate School of Veterinary Medicine, Hokkaido University.

Cell culture and transfection

HEK293 cells were cultured and transfected with the appropriate plasmid vectors as previously described (Ito *et al*., 2006).

Analysis of proteins

SDS-PAGE, immunoblotting, cell surface biotinylation, immunoprecipitation, and deglycosylation were performed as described previously (Ito *et al*., 2006; Adachi *et al*., 2009; Wang *et al*., 2012). For biotinylation, cells were washed with borate buffer (10 mM boric acid, 154 mM NaCl, 7.2 mM KCl, and 1.8 mM $CaCl_2$, pH 9.0) and were labeled with 0.8 mM sulfo-NHS-SS-biotin (Thermo Scientific) in the same buffer for 30 minutes at 4°C. The cells were rinsed with PBS containing 1 mM $CaCl_2$, 1 mM $MgCl_2$, and 100 mM glycine to quench the reaction and lysed in RIPA buffer containing 1% (w/v) deoxycholic acid, 1% (w/v) Triton X-100, 0.1% (w/v) SDS, 150 mM NaCl, 1 mM EDTA, and 10 mM Tris-HCl (pH 7.5). The cell lysate was centrifuged for 15 minutes at 20,000 × g and the supernatant was incubated with NeutrAvidin beads (Thermo Scientific) for 1 hour at 4°C to capture the biotinylated proteins. After washing with RIPA buffer, immobilized proteins were eluted in sample buffer for SDS-PAGE. For deglycosylation, proteins captured on the NeutrAvidin beads were incubated with or without endoglycosidase H (endo H) or peptide *N*-glycosidase F (PNGase) (both from Roche) in RIPA buffer. After washing the beads once, proteins were eluted in sample buffer for SDS-PAGE.

Confocal laser microscopy was performed as described previously (Ito *et al*., 2006; Adachi *et al*., 2009; Wang *et al*., 2012). In some experiments, the images were analyzed using the co-localization function of LSM5 PASCAL software to obtain Pearson's correlation coefficients to estimate the degree of co-localization between two proteins in the region of interest.

Preparation of bN[1–37]-Halo and hN[1–39]-Halo

The bait polypeptide bN[1–37]-Halo, in which the N-terminal peptide of bovine AE1 was fused to the N-terminus of the Halo-tag, was generated and used to isolate interacting proteins. The cDNA for bN[1–37] and the cDNA fragment for the Halo-tag from the pTH2 vector (Promega) were ligated into the pGEX-6P-1 vector using *Eco* RI, *Sal* I, and *Not* I restriction sites. *E. coli* BL21(DE3)pLyS competent cells (Promega) were transformed with the pGEX vector and protein expression was induced with 1 mM isopropyl-β-thiogalactopyranoside for 6 hours at 30°C. Bacterial cells were collected by centrifugation and lysed in the B-PER reagent (Thermo Scientific). GST-fused bN[1–37] in the lysate was trapped on glutathione-Sepharose beads (Amersham, Buckinghamshire, UK). Finally, bN[1–37]-Halo was cleaved from GST by the addition of Turbo 3C protease (Wako Pure Chemical Industries, Osaka, Japan) and eluted from the beads. hN[1–39]-Halo was generated using the same procedure.

Isolation and identification of proteins that interact with the N-terminus of bovine AE1 by FT-MS/MS analysis

Affinity isolation of the cellular interacting proteins was performed according to the procedure described previously (Sucic *et al*., 2011). In brief, HEK293 cells were homogenized in lysis buffer containing 50 mM Tris-HCl (pH 7.4), 0.5 mM EDTA, 1.3% (w/v) CHAPS, and 5 μg/ml aprotinin, 1 μg/ml leupeptin, 1 μg/ml pepstatin A, and 1 mM 4-(2-aminoethyl)-benzenesulfonyl fluoride (all from Sigma). The lysate was centrifuged for 1

hour at 10,000 × g and the supernatant was incubated with gentle agitation for 16 hours at 4ºC with bN[1–37]-Halo or hN[1–39]-Halo, which was immobilized on HaloLink resin (Promega). The resin was washed four times with lysis buffer containing 5 M NaCl and once with lysis buffer. Polypeptides bound to the resin were separated by SDS-PAGE on a 5–20% gradient gel (Wako Pure Chemical Industries) and stained with Coomassie brilliant blue. Polypeptides of interest were excised and subjected to reduction with dithiothreitol, alkylation with iodoacetamide, and digestion with trypsin Gold (Promega) according to the manufacturer's instructions. Tryptic peptides were separated and analyzed on a tandemly connected DIONEX Ultimate3000 liquid chromatography and LTQ Orbitrap FT-MS/MS system (Thermo Scientific). The MS/MS data were searched against the Human Database of International Protein Index using the Proteome Discoverer 1.0 (Thermo Scientific).

Binding assay for the interaction of bN[1–37]-Halo with Sec24 isoforms

The interaction of the bacterially produced bN[1–37]-Halo protein with Sec24 isoforms and Sec24C-AAA was principally analyzed as described above. Cell lysates from HEK293 cells expressing myc-tagged Sec24A, Sec24B, Sec24C, Sec24D, or Sec24C-AAA were incubated with bN[1–37]-Halo immobilized on the resin and processed as described above. Sec24 proteins bound to the resin were detected by immunoblotting using the anti-myc antibody.

Statistical analysis

Statistical significance was assessed using the paired Student's *t*-test.

Table 1. Oligonucleotide primers used in this study

Name	Target gene (GenBank Accession Number)	Sequence	Purpose
hAE1p17	Human AE1	5'-AAGCTTATGGAGGAGCTGCAGGATGAT-3'	Creation of hAE1
hAE1p2SalI	(NM 00342)	5'-GTCGACTCACACAGGCATGGCCACTTCG-3'	
hAE1pdCt11salI	Human AE1	5'-GTCGACGTATTCATCTCAACCTTCCTC-3'	Creation of hAE1Δ11
bAE1EcoRVp1	Bovine AE1 (NM101836)	5'-GACTGGTGCGTGATATCCGGC-3'	Creation of hAE1/b[1-403]
bAE1EcoRVp2		5'-GCGCCGGATATCACGCACCAG-3'	Creation of bAE1/h[1-385]
b75RsacI	Bovine AE1	5'-ATCACGAGCTCCCGCAGCTGCAC-3'	Creation of hAE1/b[1-75]
h65FscI	Human AE1	5'-GCAGGAGCTCGTGATGGACGAAAAG-3'	
b18FXbaI	Human AE1	5'-GGAGAATCTAGAGCAGGAGGAATATG-3'	Creation of hAE1/b[1-17]
h18RXbaI		5'-TCCTGCTCTAGATTCTCCTCCATC-3'	
b55REcoRV	Bovine AE1	5'-TGTGGATATCTGTGTCTGTCAGCTGGTTG-3'	Creation of hAE1/b[17-55]
h46FEcoRV	Human AE1	5'-CACAGATATCCACACACCACATCACACCCGG-3'	
b37REcoRV	Bovine AE1	5'-AATGATATCACCTTCTGCCTCTTCCATTGG-3'	Creation of hAE1/b[17-37]
h39FEcoRV	Human AE1	5'-TCACGATATCGAGGCAACAGCCCACAGAC-3'	
b37FEcoRV	Bovine AE1	5'-GATATCATTCAGGAAGAGGAGGCAG-3'	Creation of bAE1/h[18-39]
h39REcoRV	Human AE1	5'-CTCGATATCGTGAGCTGCCGGCT-3'	
bAE1H23PXbaI	Bovine AE1	5'-ACTCTAGAGCAAAAGGAATATGAAGACCCTGATTCCGT CCAGTATCCCA-3'	Creation of hAE1/b[23-37]
b17FXbaI	Bovine AE1	5'-AGACTCTAGGAGCAAAAGGAATATGAAGACC-3'	Creation of hAE1/b[25-29]
hAE1-AEGEcoRV	Human AE1	5'-ATGATATCACCTTCTGCCTCCTCCATCTGGGAC-3'	Creation of hAE1/b[33-35]
bAE1S25,27AmutF	Bovine AE1	5'-GAAGACCATGATGCCGTCGCTATCCCAATG-3'	Mutation of S25A/S27A
beAE1speIsitep5	Bovine AE1	5'-TGCAGCTGCGGGAACTAGTAATGGATGAAAAGAACC-3'	Insertion of *Spe I* site in bAE1
beAE1V26Ap1	Bovine AE1	5'-AAGACCATGATTCCGCCAGTATCCCAATGGA-3'	Mutation of V26A in bAE1
beAE1I28Ap1	Bovine AE1	5'-TCCGTCAGTGCCCCAATGGAAGAGGCAGAA-3'	Mutation of I28A in bAE1
beAE1P29Ap1	Bovine AE1	5'-TATCGCAATGGAAGAGGCAGAAGGTGACAC-3'	Mutation of P29A in bAE1
beAE1M30Ap1	Bovine AE1	5'-CCATGATTCCGTCAGTATCCCAGCAGAAGA-3'	Mutation of M30A in bAE1
beAE1V26Lp1	Bovine AE1	5'-GAAGACCATGATTCCCTCAGTATCCCAATGG-3'	Mutation of V26L in bAE1
beAE1I28Lp1	Bovine AE1	5'-GTCAGTTTGCCAATGGAAGAGGCAGAAGG-3'	Mutation of I28L in bAE1
beAE1M30Lp1	Bovine AE1	5'-CCATGATTCCGTCAGTATCCCACTCGAAGA-3'	Mutation of M30L in bAE1
beAE1SVSPIMp1	Bovine AE1	5'-CATGATTCCGTCAGTCCAATCATGGAAGA-3'	Mutation of I28P/P29I in bAE1
heAE1speIsitep5	Human AE1	5'-TGTGGAGCTGCAGGAACTAGTAATGGACGAAAAGAAC-3'	Insertion of *Spe* I site in hAE1
heAE1P27Vp2	Human AE1	5'-TCCTCCATCTGGGACTCGACGATGTCTGGG-3'	Mutation of P27V in hAE1Δ11
heAE1S29Ip1	Human AE1	5'-CCGAGATCCAGATGGAGGAGCCGGCAGCTC-3'	Mutation of S29I in hAE1Δ11
heAE1P27VS29Ip1	Human AE1	5'-GACATCGTCGAGATCCAGATGGAGGAGCCG-3'	Mutation of P27V/S29I in hAE1Δ11

(Continued from previous page)

Name	Target gene (GenBank Accession Number)	Sequence	Purpose
Ly49Ep1 Ly49Ep4	Mouse Ly49E (NM 008463)	5'-AACATACTTCATGAATTCCCACGATGAGTG-3' 5'-GTCGACACCAGGGAAATGATCCAGTTTC-3'	Cloning of Ly49E
Ly49Ep5	Mouse Ly49E	5'-ACCCACTAGTCTCACTGTGAGATCGCTT-3'	Insertion of *Spe* I site in Ly49E
beAE1/NtLy49Ep14	Bovine AE1	5'-ACGCACTAGTCCCCCGAAGAGCTT-3'	Creatiion of bN[1-37]Ly
heAE1NtLy49Ep10	Human AE1	5'-ATATCACGCACTAGTCCCCCGAAGAGCT-3'	Creation of hN[1-39]Ly
Sar1Ap1 Sar1Ap2	Human Sar1 (NM 001142648)	5'-GAATTCGCCGCCATGTCTTTCATCTTTGAG-3' 5'-CTCGAGCTACAGGTCCTCCTCTGAGATCAGCTTCTGCAT TGATGCCATGTCAATATACTGGGAGAGCCAGCGG-3'	Creation of Sar1-myc
Sar1H79Gp1	Human Sar1	5'-GTGGGGGCGAGCAAGCACGTCGCGTTTG-3'	Creation of Sar1H79G
Halotagp1 Halotagp2	pHT2 Vector	5'-GTCGACATGGGATCCGAAATCGGTACAGGC-3' 5'-GCGGCCGCTTAGCCGGCCAGCCCGGGG-3'	Cloning of Halo™-tag
bN1-37p1 bN1-37p2	Bovine AE1	5'-CCCGGGTGAATTCATGGGGGATCCGGAGG-3' 5'-GTCGACTGTGTCACCTTCTGCCTCTTCC-3'	Creation of bN[1-37]-Halo
hN1-39p1 hN1-39p2	Human AE1	5'-GGATCCGAATTCATGGAGGAGCTGCAGG-3' 5'-GTCGACTGTGTCGTGAGCTGCCGGC-3'	Creation of hN[1-39]-Halo
Sec24Ap1 Sec24Ap2	Human Sec24A (NM 021982)	5'-CTCGAGATGTCCCAGCCGGGAATACCGGCC-3' 5'-GCGGCCGCTATTTATTCACTTGTTGCTG-3'	Cloning of Sec24A
Sec24Bp1 Sec24Bp2	Human Sec24B (NM 006323)	5'-CTCGAGATGCAGGTTCCATCTGGATATGG-3' 5'-GCGGCCGCTACTTACAAATCTGCTGCTG-3'	Cloning of Sec24B
Sec24Cp1 Sec24Cp2	Human Sec24C (NM 004922)	5'-CTCGAGATGAACGTCAACCAGTCAGTTCC-3' 5'-GCGGCCGCTAGCTCAGTAGCTGCCGAATC-3'	Cloning of Sec24C
Sec24Dp1 Sec24Dp2	Human Sec24D (NM 014822)	5'-CTCGAGATGAGTCAACAAGGTTACGTGGC-3' 5'-GCGGCCGCTAATTAAGCAGCTGACAGATC-3'	Cloning of Sec24D
Sec24C-AAAp1	Human Sec24C	5'-GCGGCCGCTCCTGAGTGCATGAAGCTACTC-3'	Creation of Sec24C-AAA
mAE1p1 mAE1p2	Mouse AE1 (NM 11403)	5'-GTCGACATGGGGGACATGCGGGACCACG-3' 5'-GAATCCCATCCTAGCCATTCTCCTCGTC-3'	Creation of mouse AE1Δ11
cAE1p1 cAE1p2	Canine AE1 (AB242566)	5'-CTCGACATGGACAACCAGGACAGCACC-3' 5'-GTCGACTCAACCTTCCTCTTCATTGAAG-3'	Creation of canine AE1Δ11
eAE1p1 eAE1p2	Equine AE1 (AB242566)	5'-GTCGACCTGGATGATTCCCAGGAGAAT-3' 5'-GTCGACTTAACCTTCCTCCTCATCAAAG-3'	Creation of equine AE1Δ11
cAE1/Ly49Ep1 cAE1/Ly49Ep2	Mouse AE1	5'-CAGCCACCATGGACAACCAGGACAGCACC-3' 5'-CACTAGTGTGGGGTAAGCTACTGGCTCCTC-3'	Creation of mN[1-49]Ly
eAE1/Ly49Ep1 eAE1/Ly49Ep2	Canine AE1	5'-CAGCCACCATGGATGATTCCCAGGAGAATC-3' 5'-CACTAGACCTGGGCCTTCATAATCCTCC-3'	Creation of cN[1-46]Ly
mAE1/Ly49Ep1 mAE1/Ly49Ep2	Equine AE1	5'-CAGCCACCATGGGGGACATGCGGGACCACG-3' 5'-CACTAGTGTGGGAAGAGCTTCTGGGTC-3'	Creation of eN[1-41]Ly

Results

I. Identification of the N-terminal sequence of bovine AE1 required for its efficient cell surface expression

A portion of human erythroid AE1 N-terminally tagged with EGFP (hAE1) was detected at the cell periphery, demonstrating its cell surface expression in transfected HEK293 cells (Fig. 2). However, the C-terminal truncation mutant of hAE1 (hAE1Δ11) co-localized with calnexin, indicating that it was retained in the ER. When transfected into the same cell line, untagged hAE1 and hAE1Δ11 are reported to exhibit similar localizations to those of EGFP-hAE1 and EGFP-hAE1Δ11, respectively (Quilty *et al*., 2002). This indicates that the N-terminal EGFP tag does not have a marked effect on the intracellular distribution of hAE1 or hAE1Δ11. By contrast, EGFP-bAE1Δ11 (bAE1Δ11) and its wild-type form (bAE1) were abundantly detected at the plasma membrane (Fig. 2A). Cell surface biotinylation showed that approximately 11% and less than 3% of hAE1 and hAE1Δ11 were detected at the cell surface, respectively, whereas approximately 11% of bAE1 and bAE1Δ11 were present at the cell surface (Fig. 2B), confirming our previous observations (Adachi *et al*., 2009). These data indicate that a mechanism serves to deliver bAE1 to the cell surface, which is unaffected by the presence or absence of the 11 C-terminal amino acid residues.

We examined the intracellular localization of bAE1Δ11 and hAE1Δ11 chimeric proteins (Fig. 3). The hAE1Δ11 chimera, whose N-terminal cytoplasmic domain was replaced with that of bAE1 (hAE1Δ11/b[1–403]), showed plasma membrane localization (Fig. 4). By

contrast, cell surface expression of bAE1Δ11 was markedly reduced by substitution of its cytoplasmic domain with that of hAE1, resulting in the retention of bAE1Δ11/h[1–385] in the ER. Thus, the key signal responsible for the plasma membrane targeting of bAE1 is present in the cytoplasmic domain. Subsequent microscopic and biotinylation studies on a series of chimeric AE1 proteins (Figs. 4 and 5) demonstrated that a portion of both hAE1/b[25–29] and its Δ11 mutant were expressed at the plasma membrane (Fig. 5). This demonstrates that replacement of the ^{26}IPESQ^{30} sequence with the corresponding ^{25}SVSIP^{29} bovine sequence is sufficient to facilitate effective targeting of hAE1 and hAE1Δ11 to the plasma membrane. This was further supported by the loss of cell surface expression and ER retardation of bAE1 and bAE1Δ11 when their ^{25}SVSIP^{29} sequence was replaced with ^{26}IPESQ^{30} (bAE1/h[26–30], Fig. 5).

We next generated a series of mutants of bAE1 and hAE1Δ11 possessing substitutions of certain amino acid residues in ^{25}SVSIP^{29} and neighboring positions (Fig. 6) and examined their cell surface expression by microscopy and biotinylation (Fig. 7). Alanine substitution of Ser^{25}, Ser^{27}, or Pro^{29} had no effect on the plasma membrane expression of bAE1 (Figs. 6 and 7). Alanine substitution of Val^{26} and Ile^{28} resulted in the ER retention of these proteins and they were no longer detected at the cell surface, whereas replacement of these residues with leucine or phenylalanine did not alter the localization. Similarly, substitution of Met^{30}, the C-terminal neighboring residue of ^{25}SVSIP^{29}, with alanine markedly reduced the surface expression of AE1, whereas substitution with leucine did not. Moreover, the protein was not detected at the cell surface following mutation of ^{28}IP^{29} to ^{28}PI^{29}.

Similarly, the cell surface expression of hAE1Δ11/P27V/S29I, in which the Pro^{27} and Ser^{29} residues of ^{26}IPESQ^{30} were mutated to valine and isoleucine, respectively, was markedly increased compared with that of hAE1Δ11, whereas no effect was observed when either of these residues was mutated individually (Fig. 8A). The intracellular fractions of hAE1Δ11/P27V and hAE1Δ11/S29I were sensitive to digestion with endo H (Fig. 8B), confirming their ER localization as indicated by co-localization with calnexin (Fig. 8A). By contrast, the cell surface fraction of hAE1Δ11/P27V/S29I was resistant to endo H, demonstrating its targeting to the plasma membrane through the Golgi apparatus, although a small portion of the intracellular fraction of this mutant was sensitive to endo H (Fig. 8B). These data demonstrate that the (V/L/F)X(I/L)X(M/L) sequence (^{26}VSIPM^{30} in bovine AE1) at this position, which corresponds to a ΦXΦXΦ sequence, facilitates the plasma membrane targeting of AE1 and AE1Δ11 and suggests that this motif increases the ER-Golgi transport of these proteins.

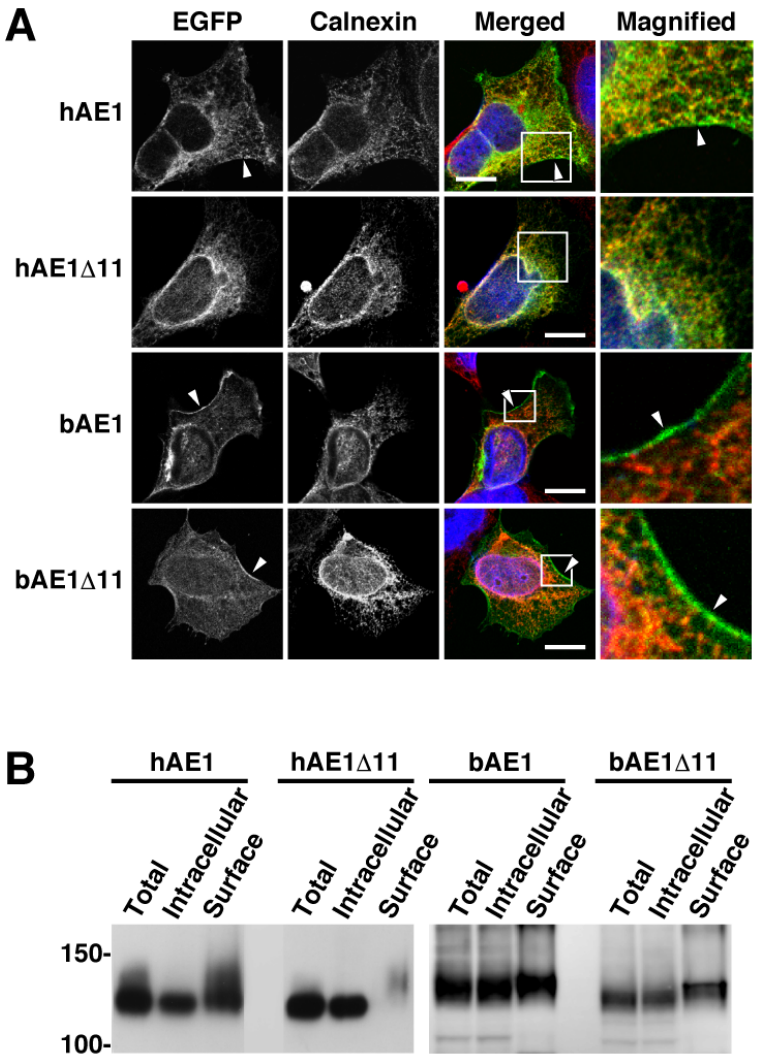

Figure 2. Expression of human and bovine AE1 and their C-terminally truncated mutants in transfected HEK293 cells. *A*, HEK293 cells were transfected with EGFP-tagged hAE1 or bAE1 and their C-terminally truncated mutants hAE1Δ11 and bAE1Δ11, respectively. Cells were fixed after 48 hours, and EGFP and the ER marker calnexin were visualized. A merged image of EGFP (*green*), calnexin (*red*), and DAPI-stained nuclei (*blue*) is shown. The indicated areas in the merged images are magnified and arrowheads indicate EGFP fluorescence at the plasma membrane. Bars, 10 μm. *B*, At 48 hours after transfection, cell surface proteins were labeled with sulfo-NHS-SS-biotin. After solubilization, biotin-labeled proteins were separated from intracellular proteins on NeutrAvidin beads. AE1 proteins in total (*Total*), Intracellular (*Intracellular*), and cell surface (*Surface*) fractions were detected by immunoblotting with an anti-GFP antibody. The amount of cell surface fraction loaded is 10-fold higher than that of the other fractions. Migrating positions of size markers are shown in kDa.

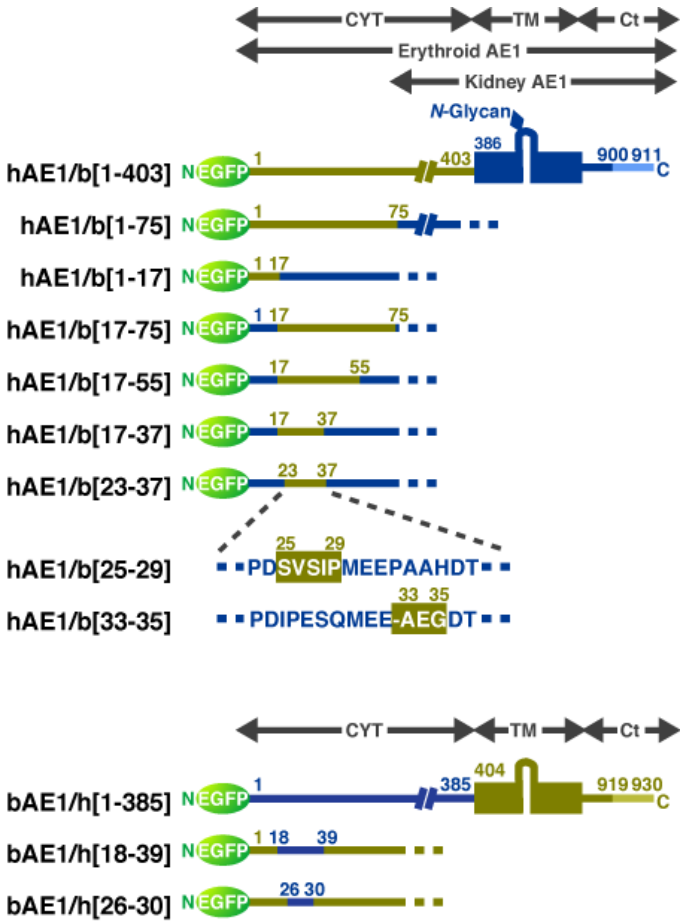

Figure 3. Schematic illustration for a series of bAE1 and hAE1 chimeric proteins. A series of bAE1 and hAE1 chimeric proteins are schematically illustrated with the numbers of the amino acid residues shown. The overall structures of erythroid and kidney AE1 are presented along with a representative illustration of the hAE1/b[1–403] mutant. *CYT*, *TM*, and *Ct* indicate the cytoplasmic domain, the transmembrane domain, and the short C-terminal cytoplasmic tail, respectively. The chimeras hAE1/b[1–403], hAE1/b[1–75], hAE1/b[1–17], hAE1/b[17–75], hAE1/b[17–55], hAE1/b[17–37], hAE1/b[23–37], hAE1/b[25–29], and hAE1/b[33–35] have a hAE1 backbone and contain amino acid residues 1–403, 1–75, 1–17, 17–75, 17–55, 17–37, 23–37, 25–29, and 33–35 from bAE1, respectively. Conversely, the chimeras bAE1/h[1–385], bAE1/h[18–39], and bAE1/h[26–30] contain the N-terminal amino acid residues 1–385, 18–39, and 26–30 of hAE1, respectively, in the corresponding regions of bAE1. The Δ11 mutants of these chimeras, in which the 11 C-terminal amino acid residues were deleted, were also prepared. hAE1 has a single *N*-gycosylation site on the fourth extracellular loop in the TM, whereas bAE1 does not (Ito *et al*., 2006).

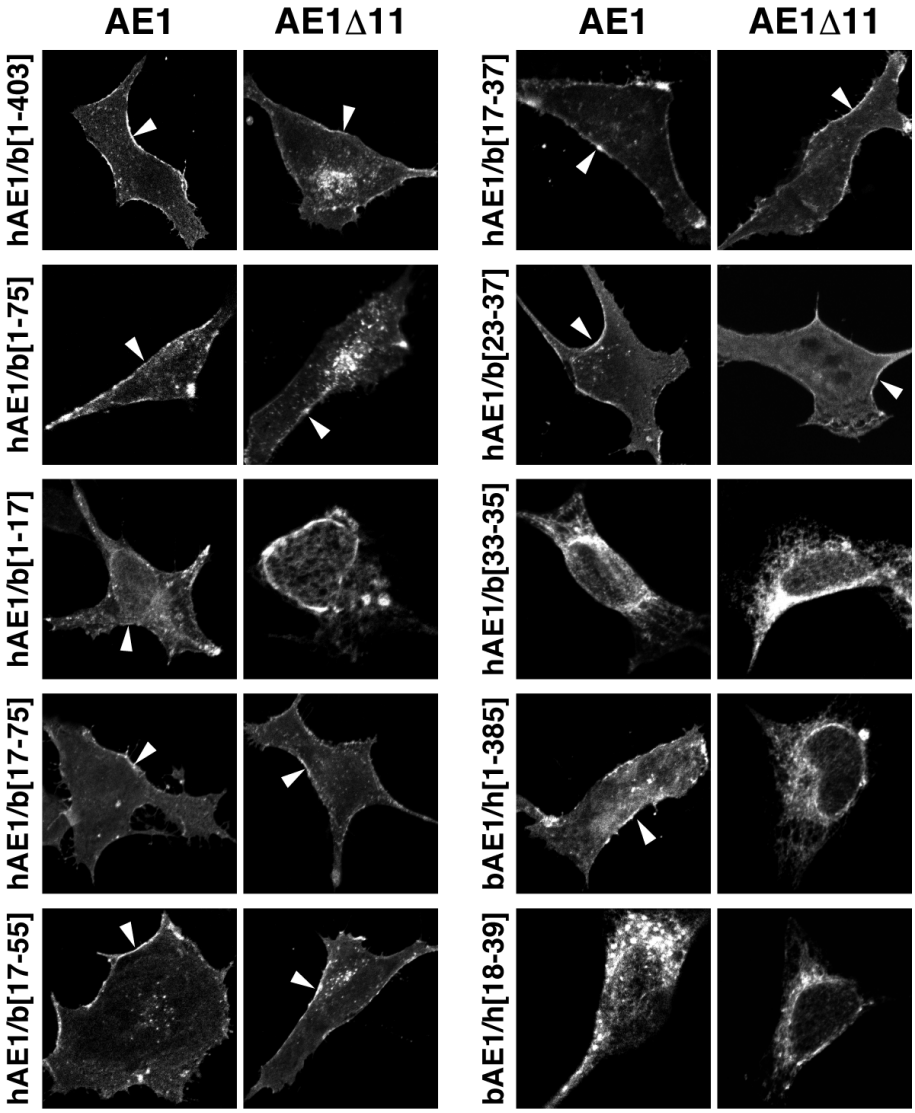

Figure 4. Intracellular localization of a series of bAE1-hAE1 chimeric proteins and their Δ11 mutants. Various bAE1-hAE1 chimeras and their Δ11 mutants (illustrated in Fig. 3) were transfected into HEK293 cells and their intracellular localizations were determined by confocal laser microscopy. EGFP fluorescence at the plasma membrane is indicated by arrowheads.

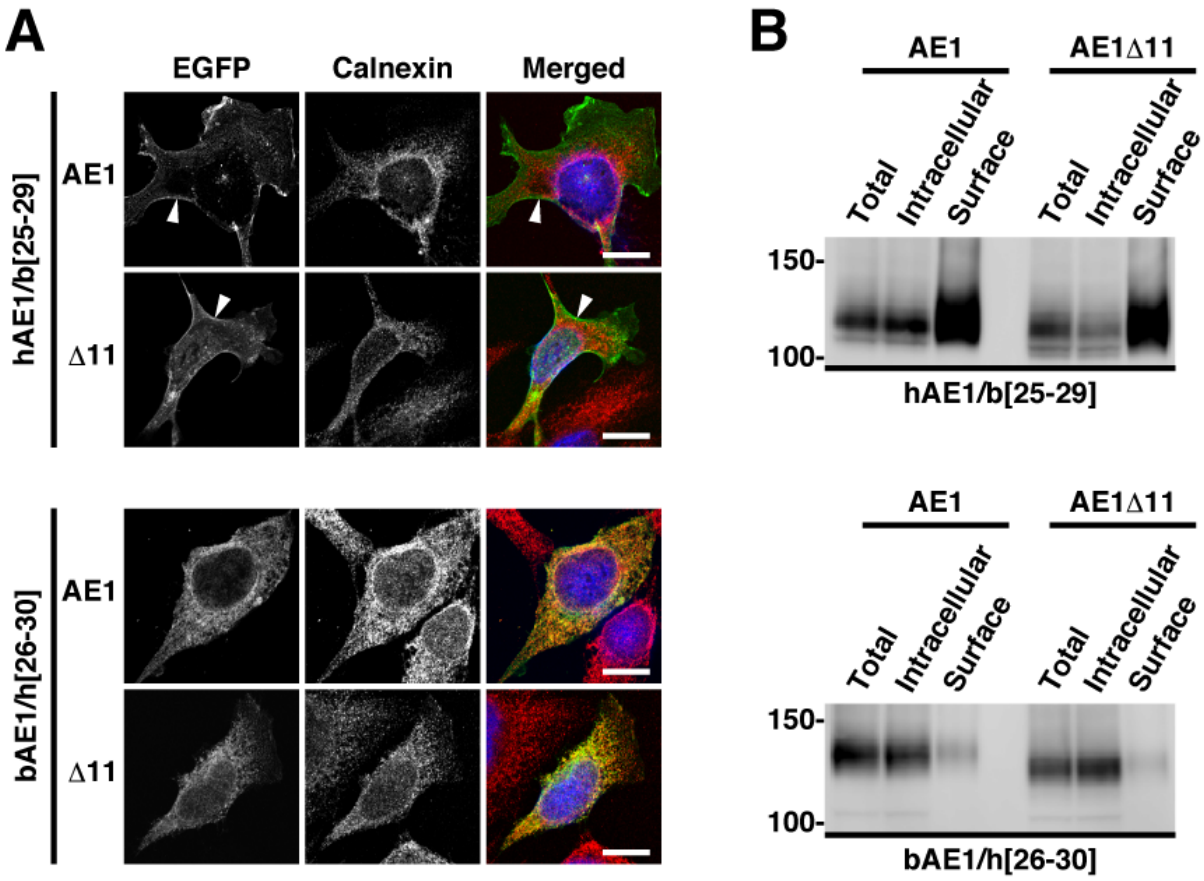

Figure 5. Intracellular distribution of hAE1/b[25–29] and bAE1/h[26–30] chimeric proteins and their Δ11 mutants. *A*, HEK293 cells were transfected with EGFP-hAE1/b[25–29], EGFP-bAE1/h[26–30], and their Δ11 mutants. Cells were fixed at 48 hours after transfection and stained with an anti-calnexin antibody. Arrowheads indicate EGFP fluorescence at the cell surface. EGFP (*green*), calnexin (*red*), and DAPI-stained nuclei (*blue*) are shown in the merged images. Bars, 10 μm. B, Cell surface expression of hAE1/b[25–29], bAE1/h[26–30], and their Δ11 mutants was examined by cell surface biotinylation as described in the legend for Fig. 2. AE1 proteins in the total (*Total*), intracellular (*Intracellular*), and cell surface (*Surface*) fractions were detected by immunoblotting using an anti-GFP antibody. The amount of cell surface fraction loaded is 10-fold higher than that of the other fractions. The migrating positions of the size markers are shown in kDa.

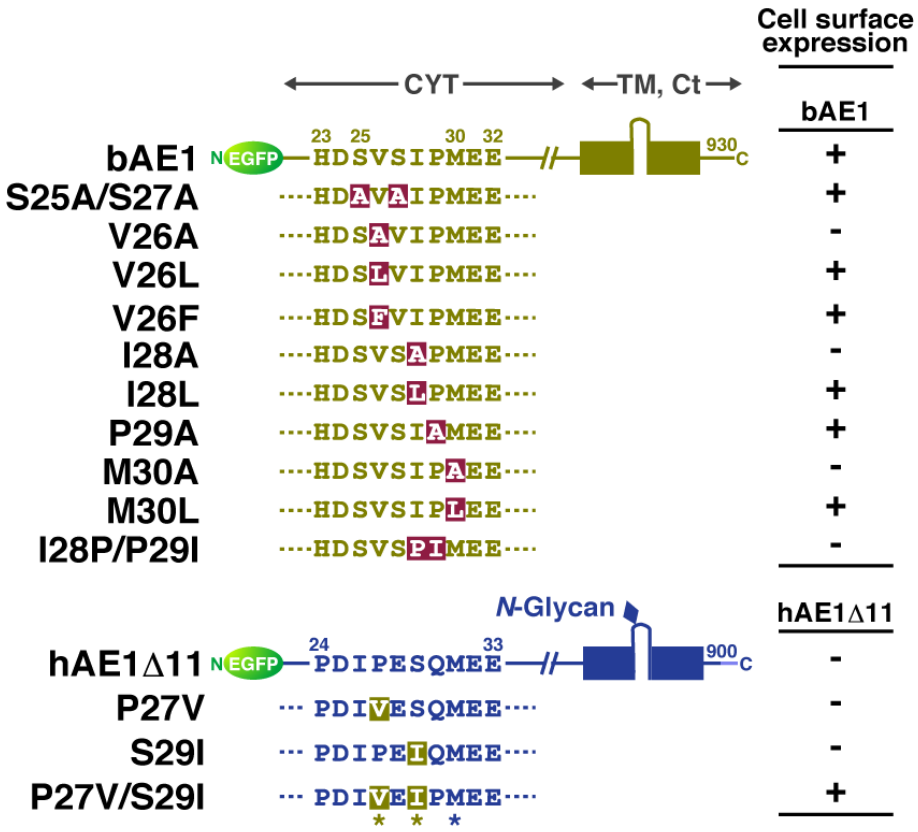

Figure 6. Diagram of various amino acid substitution mutants of AE1 and the summary for their intracellular distributions. Various amino acid substitution mutants of EGFP-bAE1 and EGFP-hAE1Δ11 were transfected into HEK293 cells. Mutated amino acid residues are highlighted. The cell surface expression of these mutants, as determined by laser confocal microscopy and cell surface biotinylation studies (Figs. 7 and 8), is summarized by + and − indicating positive and negative (less than 5% of the total amount) cell surface expression, respectively. *CYT*, *TM*, *Ct* indicate the N-terminal cytoplasmic domain, the transmembrane domain, and the short cytoplasmic C-terminal tail, respectively. bAE1 is not *N*-glycosylated (Ito *et al*., 2006), whereas hAE1 possesses a single *N*-glycan in the extracellular loop.

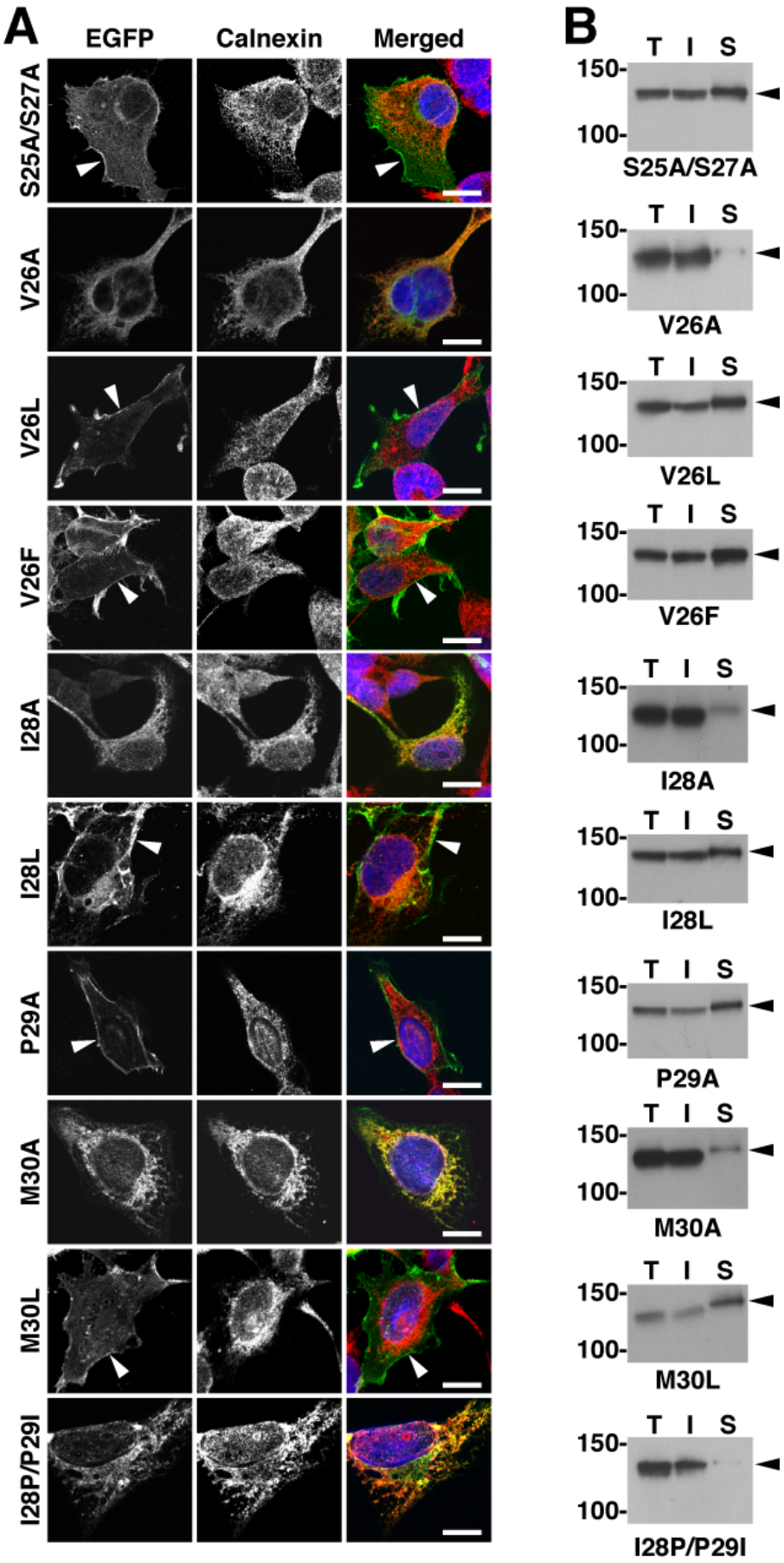
A
EGFP
Calnexin
Merged
S25A/S27A
V26A
V26L
V26F
I28A
I28L
P29A
M30A
M30L
I28P/P29I
B
T I S
150-
100-
S25A/S27A
V26A
V26L
V26F
I28A
I28L
P29A
M30A
M30L
I28P/P29I

(Previous page)

Figure 7. Intracellular localizations of the amino acid substitution mutants of EGFP-bAE1. HEK293 cells were transfected with various EGFP-bAE1 mutants in which one or two amino acid residues in the ^{25}SVSIPM^{30} sequence were substituted by the indicated residue(s). After 48 hours, the intracellular localizations of the mutants were analyzed by confocal laser microscopy (*A*) and cell surface biotinylation (*B*), as described in the legend of Fig. 2. In *A*, EGFP fluorescence at the plasma membrane is indicated by arrowheads. EGFP (*green*), calnexin (*red*), and DAPI-stained nuclei are shown in the merged images. Bars, 10 μm. In B, bAE1 mutants detected by immunoblotting of the total (*T*), intracellular (*I*), and cell surface (*S*) fractions are shown, and the migrating positions of the size markers are shown in kDa. Cell surface expression of each mutant was determined by the presence of EGFP fluorescence at the plasma membrane (*A*) and when the relative abundance of the mutant in the cell surface fraction comprised more than 5% of the total amount, as determined by densitometric scanning of the immunoblots (*B*).

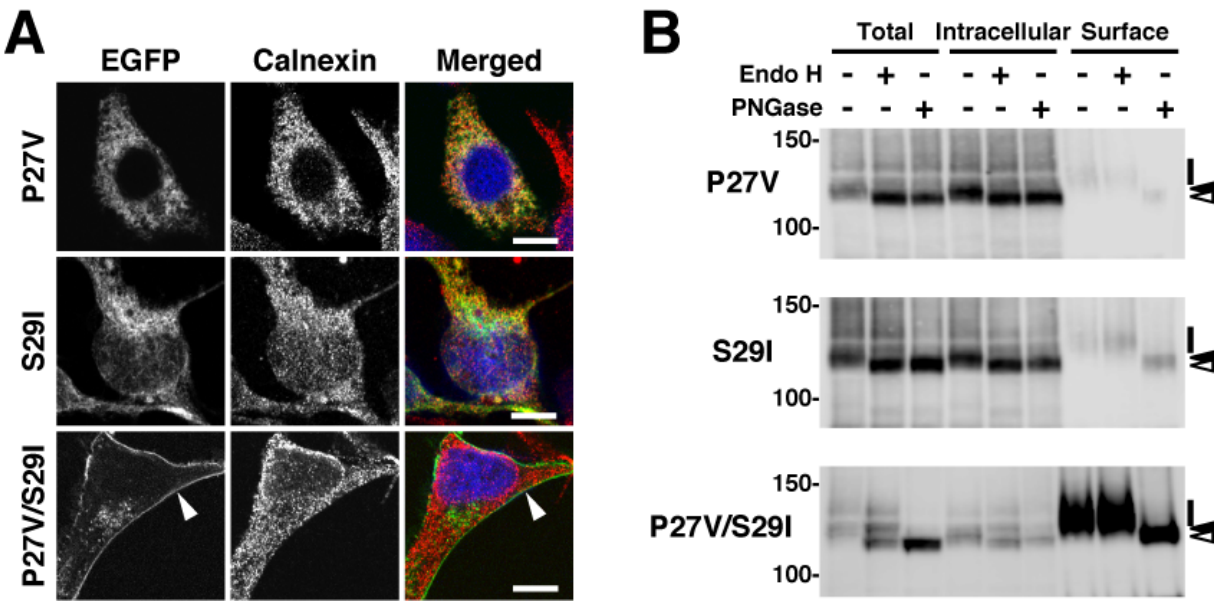

Figure 8. Cell surface expression and *N*-glycan maturation of hAE1Δ11 mutants with the ΦXΦXΦ sequence in its N-terminus. Intracellular localization of hAE1Δ11/P27V, hAE1Δ11/S29I, and hAE1Δ11/P27V/S29I were examined by confocal laser microscopy (*A*) and cell surface biotinylation (*B*) as described in the legend to Fig. 2. EGFP fluorescence at the plasma membrane is indicated by arrowheads in *A*. Bars, 10 μm. Total (*Total*), intracellular (*Intracellular*) and cell surface (*Surface*) fractions were deglycosylated with endo H or PNGase. The amount of cell surface fraction loaded is 10-fold higher than that of the other fractions. Symbols indicate the migrating positions of each hAE1Δ11 mutant with mature and processed *N*-glycan (*bars*), endo H-sensitive immature *N*-glycans (*closed arrowheads*), and the deglycosylated polypeptides (*open arrowheads*). The migrating positions of the size markers are shown in kDa.

II. Identification of the ΦXΦXΦ sequence as an ER export signal

To verify this hypothesis, we first examined if the insertion of the ΦXΦXΦ sequence was sufficient to induce the plasma membrane targeting of another protein. For this purpose, we used Ly49E, a type II transmembrane protein consisting of a short cytoplasmic N-terminus, a single transmembrane α-helix, and a large extracellular C-terminal lectin-like domain (Van Beneden *et al*., 2001; Yokoyama and Plougastel, 2003), as a reporter protein. Three potential *N*-glycosylation sites in Ly49E meant different forms of the protein with mature processed *N*-glycan or with immature core *N*-glycan could be distinguished. The redistribution of Ly49E has been monitored following replacement of its N-terminus with that of the human CLC-4 chloride channel (Okkenhaug *et al*., 2006).

We created reporter proteins containing the Ly49E backbone and a C-terminal EGFP tag, namely bN[1–37]Ly, hN[1–39]Ly, and hN[P27V/P29I]Ly, whose N-terminal cytoplasmic regions were replaced by the N-terminal 1–37 residues of bAE1, residues 1–39 of hAE1, or residues 1–39 of hAE1 containing the P27V/P29I mutation, respectively (Fig. 9). Approximately 17% and 18% of the total amount of bN[1–37]Ly and hN[P27V/S29I]Ly expressed in HEK293 cells was biotinylated at the cell surface, respectively, and they principally consisted of polypeptides of 63–73 kDa (Fig. 10A) whose *N*-glycan was resistant to endo H (Fig. 10B). By contrast, the vast majority of hN[1–39]Ly was 60 kDa in size, intracellular, and completely sensitive to endo H digestion. Microscopic analysis showed that bN[1–37]Ly and hN[P27V/S29I]Ly were localized at the plasma membrane with some juxtanuclear signals, whereas hN[1–39]Ly exhibited a reticular pattern that was consistent

with calnexin (Fig. 11). hN[1–39]Ly partially co-localized with Sec23A and ERGIC53, which are markers of ER exit sites and the ERGIC, respectively, in juxtanuclear areas, but did not co-localize with GM130, a marker of the *cis*-Golgi.

An activated form of Sar1A, Sar1A H79G, inhibits the formation of COPII-coated vesicles (Aridor *et al*., 1995). We analyzed the effect of Sar1A H79G on the *N*-glycan processing of AE1-Ly49E mutants (Fig. 12). Co-expression of myc-tagged wild-type Sar1A had no significant effect on the relative abundance of bN[1–37]Ly, hN[1–39]Ly, or hN[P27V/S29I]Ly with mature *N*-glycan, although the value for hN[1–39]Ly (17% ± 4%, n = 3) was much lower than that for bN[1–37]Ly (74% ± 4%, n = 3) and hN[P27V/S29I]Ly (68% ± 4%, n = 3). However, when Sar1A H79G was co-transfected, the relative abundance of the mature forms of bN[1–37]Ly and hN[P27V/S29I]Ly was markedly reduced to less than 5% of the total amount. This indicates that bN[1–37]Ly and hN[P27V/S29I]Ly were transported to the cell surface via the conventional secretory pathway.

These data demonstrate that the N-terminal segments bN[1–37] and hN[P27V/S29I] can induce effective ER export of the Ly49E reporters through the COPII pathway, and that the P27V/S29I substitution, *i.e*., creation of the ΦXΦXΦ motif, significantly increased the basal level of hN[1–39]Ly ER exit. Therefore, we next tested whether hydrophobic clusters of AE1 proteins from several other species that contain a ΦXΦXΦ motif behave as the bovine sequence does. When transfected into HEK293 cells, equine and murine AE1Δ11 mutants that contain ^{11}IEVIV^{15} and ^{35}LTIPV^{39} in the N-terminal stretches, respectively, were found at the plasma membrane, whereas canine AE1Δ11, which lacks an N-terminal ΦXΦXΦ

sequence, was retained in the ER (Fig. 13, also see Fig. 1). Moreover, chimeras containing the first 41 or 49 amino acids of equine or murine AE1, respectively, and the transmembrane and C-terminal regions of Ly49E exhibited effective cell surface expression and endo H-resistant *N*-glycans, whereas a chimera possessing the 46 N-terminal residues of canine AE1 was primarily unprocessed and was not detected at the cell surface (Fig. 14). Based on these findings, we conclude that the ΦXΦXΦ motif facilitates the ER export of membrane proteins.

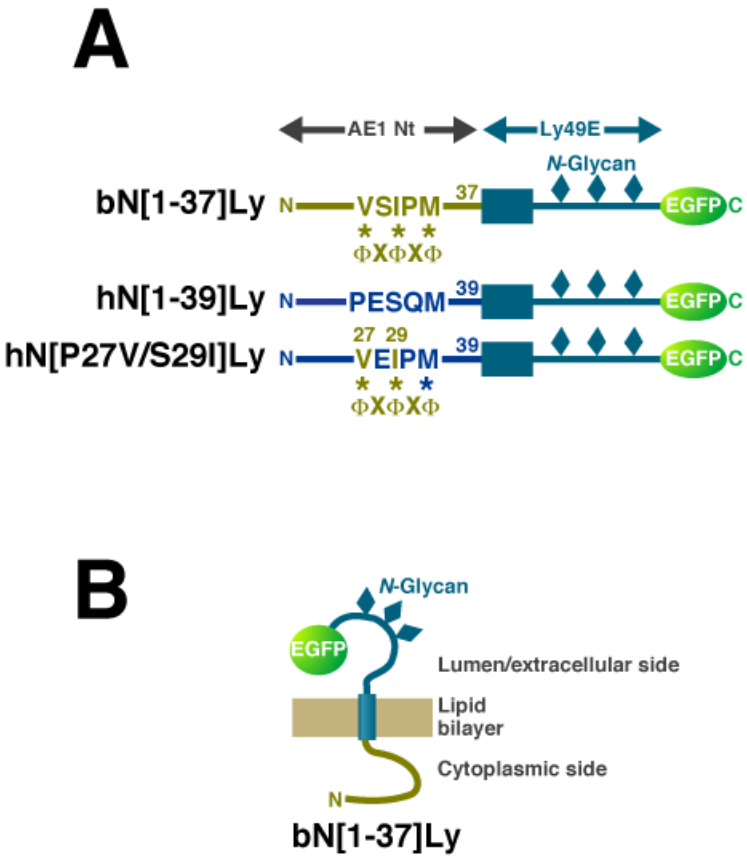

Figure 9. Schematic illustration of the AE1-Ly49E chimeric reporter proteins. Schematic illustration of the AE1 N-terminus-Ly49E chimeric proteins (*bN[1–37]Ly*, *hN[1–39]Ly*, and *hN[P27V/S29I]Ly*), which contain the N-terminal cytoplasmic regions (*AE1 Nt*) of bAE1, hAE1, or hAE1/P27V/S29I and the transmembrane and extracellular domains of Ly49E with an N-terminal EGFP tag. *B* shows the schematic illustration for bN[1–37]Ly embedded in the lipid bilayer.

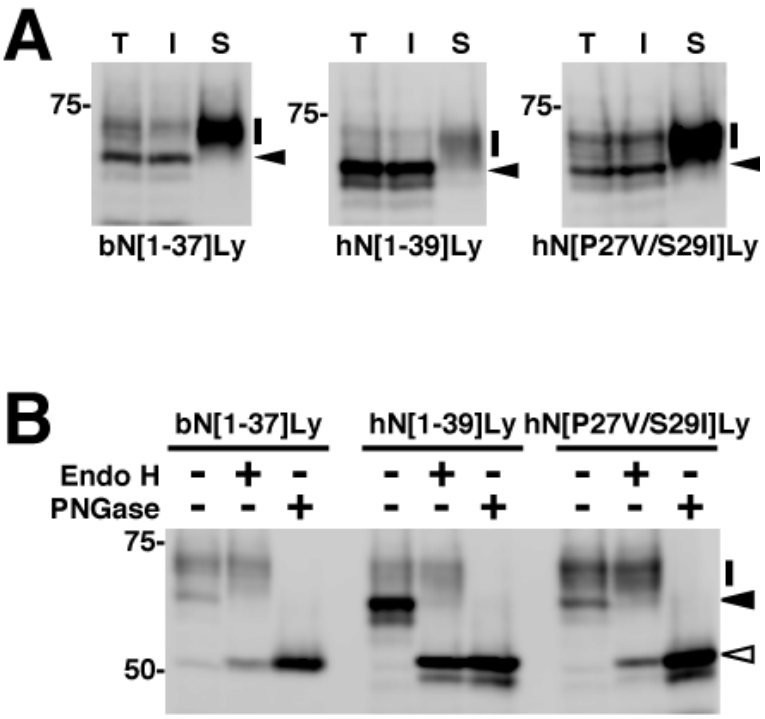

Figure 10. Cell surface expression and *N*-glycan maturation of the AE1-Ly49E mutants. AE1-Ly49E were transfected into HEK293 cells and the intracellular localizations were analyzed by biotinylation (*A*) and deglycosylation (*B*) as described in the legends for Figs. 2 and 8. A representative immunoblot of three independent experiments is presented in *B*. *T*, *I*, and *S* indicate the total, intracellular, and cell surface fractions, respectively. The amount of cell surface fraction loaded is 10-fold higher than that of the other fractions. Bars, closed arrowheads, and open arrowheads indicate the migrating positions of the mutant proteins whose *N*-glycan is endo H-resistant, endo H-sensitive, and deglycosylated, respectively. The migrating positions of the size markers are shown in kDa.

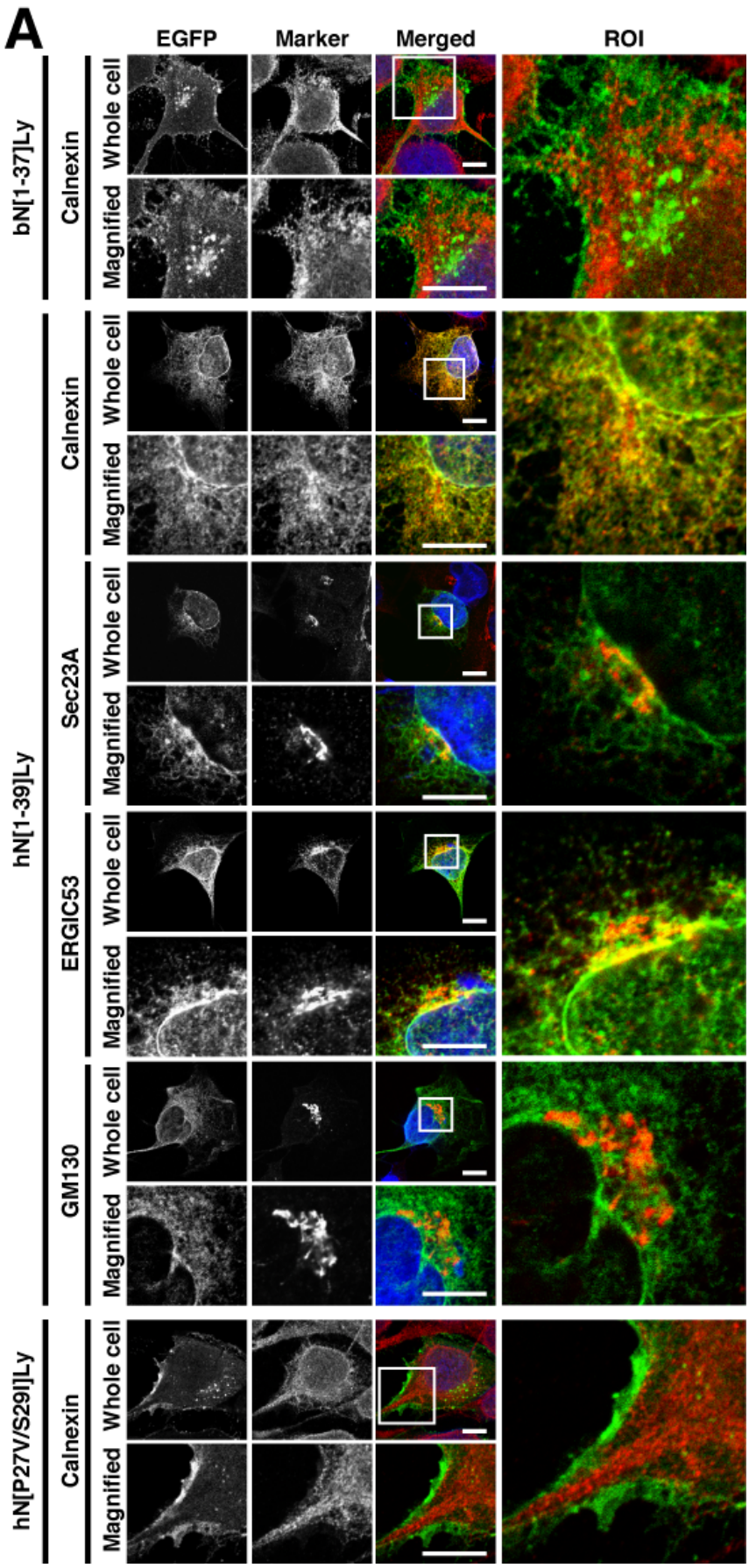
A
EGFP
Marker
Merged
ROI
bN[1-37]Ly
hN[1-39]Ly
hN[P27V/S29I]Ly
Calnexin
GM130
ERGIC53
Sec23A
Whole cell
Magnified

(Continued from previous page)

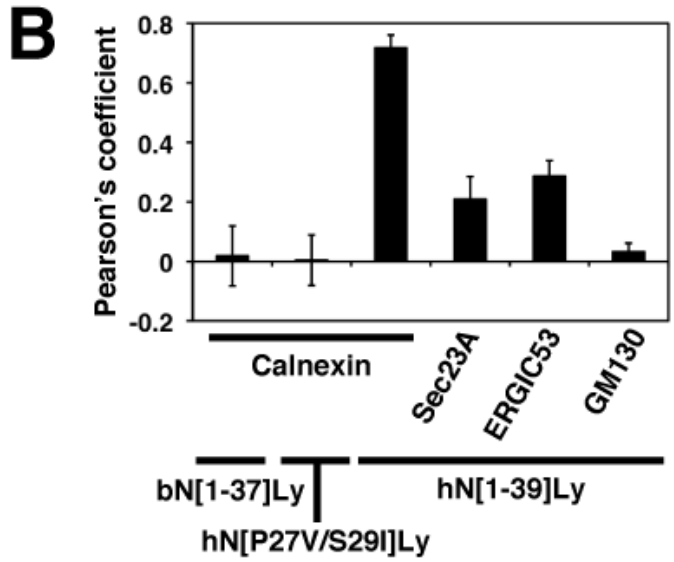

Figure 11. Intracellular distribution of the AE1-Ly49E chimeric proteins in transfected HEK293 cells. In A, EGFP fluorescence (*green*) was visualized in HEK293 cells expressiong bN[1–37]Ly, hN[1–39]Ly, or hN[P27V/S29I]Ly. The ER, ER exit sites, ERGIC and *cis*-Golgi were stained with anti-calnexin, anti-Sec23A, anti-ERGIC53, and anti-GM130 antibodies, respectively (*red*). Representative images are shown. The indicated areas of the region of interest in the merged images are magnified (*Magnified* and *ROI*). Bars, 10 μm. In *B*, Pearson's coefficients of co-localization between AE1-Ly49E chimeric proteins and organelle markers were analyzed. Co-localization was analyzed for each marker in the regions of interest of 24 cells using LSM5 PASCAL co-localization software. Data are shown as the mean ± S.D. (n = 24).

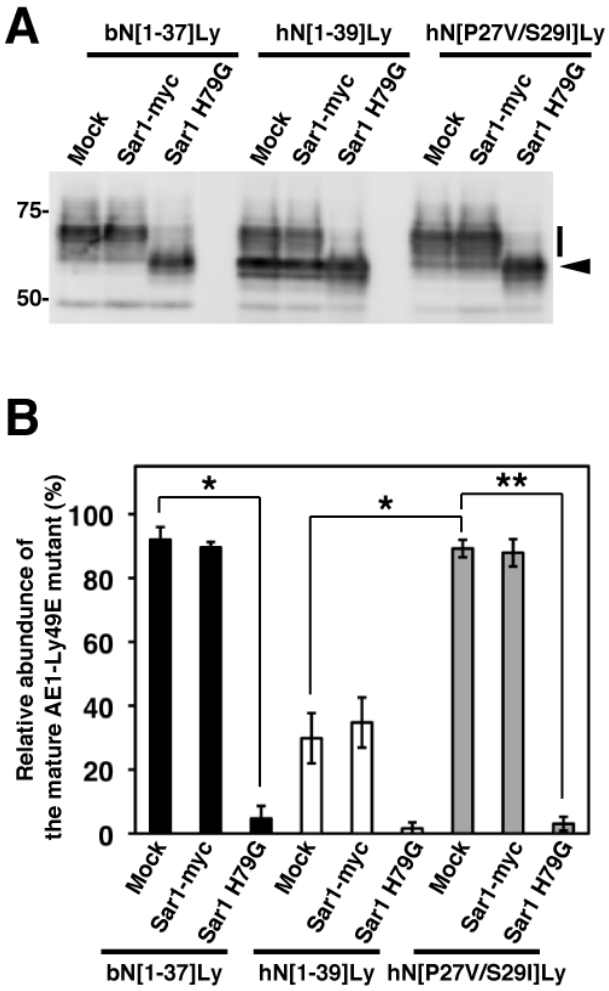

Figure 12. Effect of Sar1A expression on the *N*-glycan processing of AE1-Ly49E reporter proteins. A, HEK293 cells were co-transfected with a AE1-Ly49E mutant (*bN[1–37]Ly*, *hN[1–39]Ly*, or *hN[P27V/S29I]Ly*) and either an empty vector (*Mock*), C-terminally myc-tagged Sar1A (*Sar1-myc*), or its activated form (*Sar1 H79G*). After 48 hours of incubation, cell lysates were prepared and AE1-Ly49E mutants were detected by immunoblotting with an anti-GFP antibody. A representative immunoblot from three independent experiments is presented. Bars and arrowheads indicate the migrating positions of AE1-Ly49E mutants with mature and immature *N*-glycans, respectively. The migrating positions of the size markers are shown in kDa. B, The abundance of the AE1-Ly49E mutants bearing mature *N*-glycans relative to the total amount was quantitated by densitometric scanning of the immunoblots. Data are expressed as the mean ± S.D. (n = 3, *p<0.05, **p<0.005).

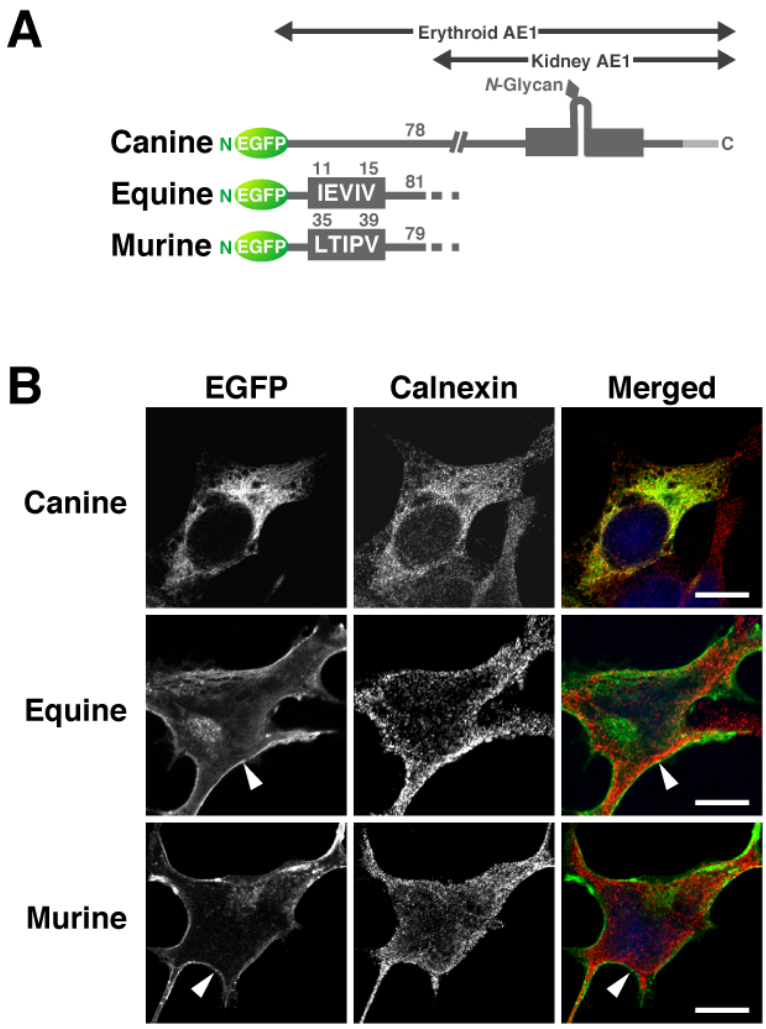

Figure 13. Roles of the N-terminal sequence of erythroid AE1 from several species in cell surface expression of the proteins. *A*, Schematic illustration of EGFP-tagged AE1Δ11 mutants of canine, equine, and murine erythroid AE1. Equine and murine erythroid AE1 contain the N-terminal sequences ^{11}IEVIV^{15} and ^{35}LTIPV^{39}, which conform to the ΦXΦXΦ motif, respectively, whereas canine erythroid AE1 does not contain this motif as shown in Fig. 1. *B*, EGFP-AE1Δ11 mutants described above were transfected into HEK293 cells, which were then fixed and stained for calnexin. Equine and murine AE1Δ11 were abundant at the plasma membrane (*arrowheads*), whereas canine AE1Δ11 exhibited a similar pattern to calnexin. EGFP (*green*), calnexin (*red*), and DAPI-stained nuclei (*blue*) are shown in the merged images. Bars, 10 μm.

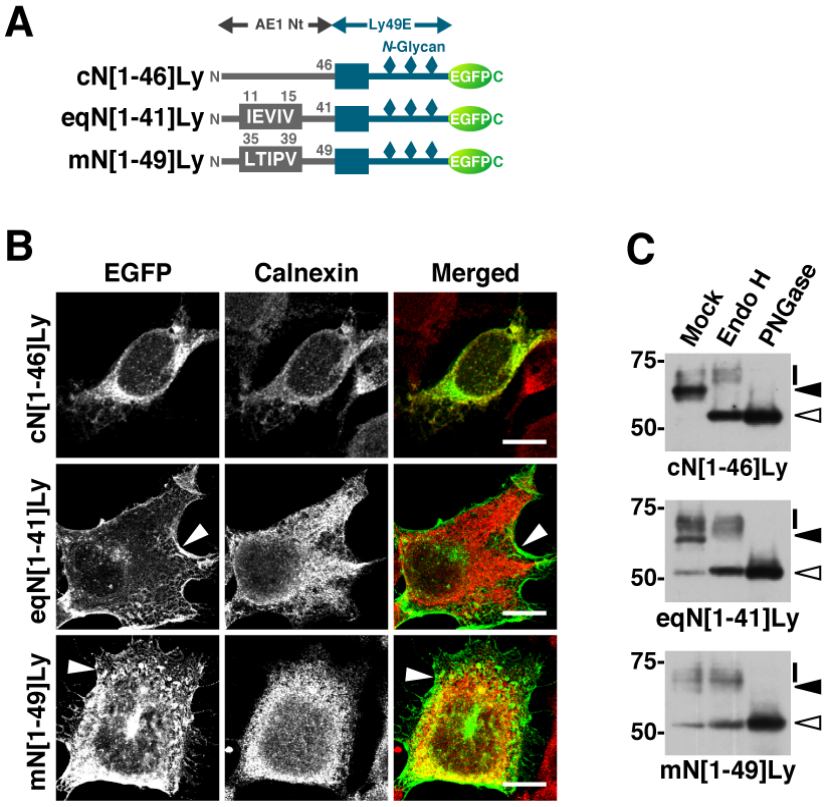

Figure 14. Intracellular localization and the *N*-glycan processing of the AE1-Ly49E chimeric proteins containing the N-terminal sequences of canine, equine, and murine erythroid AE1. *A*, The partial sequences of the N-terminal regions of canine, equine, and murine erythroid AE1 (*AE1 Nt*) were substituted for the N-terminal cytoplasmic region of Ly49E to create the AE1-Ly49E chimeric proteins cN[1–46]Ly, eqN[1–41]Ly, and mN[1–49]Ly, respectively. *B* and *C*, HEK293 cells were transfected with cN[1–46]Ly, eqN[1–41]Ly, and mN[1–49]Ly, and incubated for 48 hours. The intracellular localizations of the mutants were examined by confocal laser microscopy after staining with an anti-calnexin antibody (*B*) and *N*-glycan processing was analyzed by deglycosylation as described in the legends to Figs. 2 and 8 (*C*). In *B*, the plasma membrane expression of eqN[1–41]Ly and mN[1–49]Ly is indicated by arrowheads. Bars, 10 μm. In *C*, total cell lysates from the transfected cells were mock-treated, endo H-treated, or PNGase-treated, and then immunoblotted with an anti-EGFP antibody. The migrating positions of each AE1-Ly49E mutant with mature and processed *N*-glycans (*bars*), endo H-sensitive immature *N*-glycans (*closed arrowheads*), and the deglycosylated polypeptides (*open arrowheads*) are indicated. The migrating positions of the size markers are shown in kDa.

III. Selective interaction of the ΦXΦXΦ motif with Sec24C

These findings suggest that some COPII components, or other adaptor proteins, interact with the ΦXΦXΦ sequence upon ER exit. To identify the interacting protein(s), we isolated proteins that specifically bound to the motif from HEK293 cell lysates using bN[1–37]-Halo-tag fusion proteins as the bait. Two polypeptides of 120-kDa and 85-kDa were identified, which bound to bN[1–37]-Halo, but not to hN[1–39]-Halo (Fig. 15A). MS/MS analysis of these bands and a database search identified the 120-kDa and 85-kDa proteins as human Sec24C and Sec23A, respectively (Table 2). Moreover, the 85-kDa polypeptide reacted specifically with an anti-Sec23A antibody on immunoblots (Fig. 15B). In the Sec23/Sec24 complex, Sec24 is the primary cargo selection element (Miller *et al*., 2003; Mossessova *et al*., 2003; Bonifacino and Glick, 2004) and two mammalian paralogues of Sec23, Sec23A and Sec23B, serve distinct functions, probably due to their differential tissue-specific expression (Zanetti *et al*., 2012). Therefore, we hereafter focused on Sec24C in this study.

Using the same procedure, we tested the interaction between bN[1–37]-Halo and myc-tagged Sec24A, Sec24B, Sec24C, or Sec24D by overexpressing these proteins in HEK293 cells to determine the specificity of bN[1–37]-Halo for the Sec24 isoforms. Sec24C bound to bN[1–37], whereas the other isoforms did not. In addition, the Sec24C-AAA mutant, in which the ^{895}LIL^{897} sequence that forms the binding pocket for the IXM motif on membrin and syntaxin 5 (Mancias and Goldberg, 2008) was changed to ^{895}AAA^{897}, did not bind bN[1–37] (Fig. 16). Furthermore, when the Sec24C-AAA mutant was co-transfected with the

AE1-Ly49E chimeras, the abundance of the immature forms of bN[1–37] and hN[P27V/S29I] relative to the total amount was significantly higher than when they were mock co-transfected. By contrast, co-transfection of the Sec24C-AAA mutant caused no significant change in the abundance of the immature form of VSV-G, which interacts with Sec24A/Sec24B (Nishimura and Balch, 1997) (Fig. 17). There was no marked change in the relative abundance of the immature form of the chimeras in cells expressing wild-type Sec24C compared with that in mock-treated cells (Fig. 17). Thus, the presence of Sec24C-AAA reduced the ER export of bN[1–37]Ly and hN[P27V/S29I]Ly, which both contain the ΦXΦXΦ motif, indicating that the motif interacts with this region of Sec24C.

These findings demonstrate that the ΦXΦXΦ motif interacts with the Sec23A/Sec24C complex by specifically binding to ^{895}LIL^{897} on the surface of Sec24C, and that this interaction potently increases the efficiency of ER export of cargo proteins.

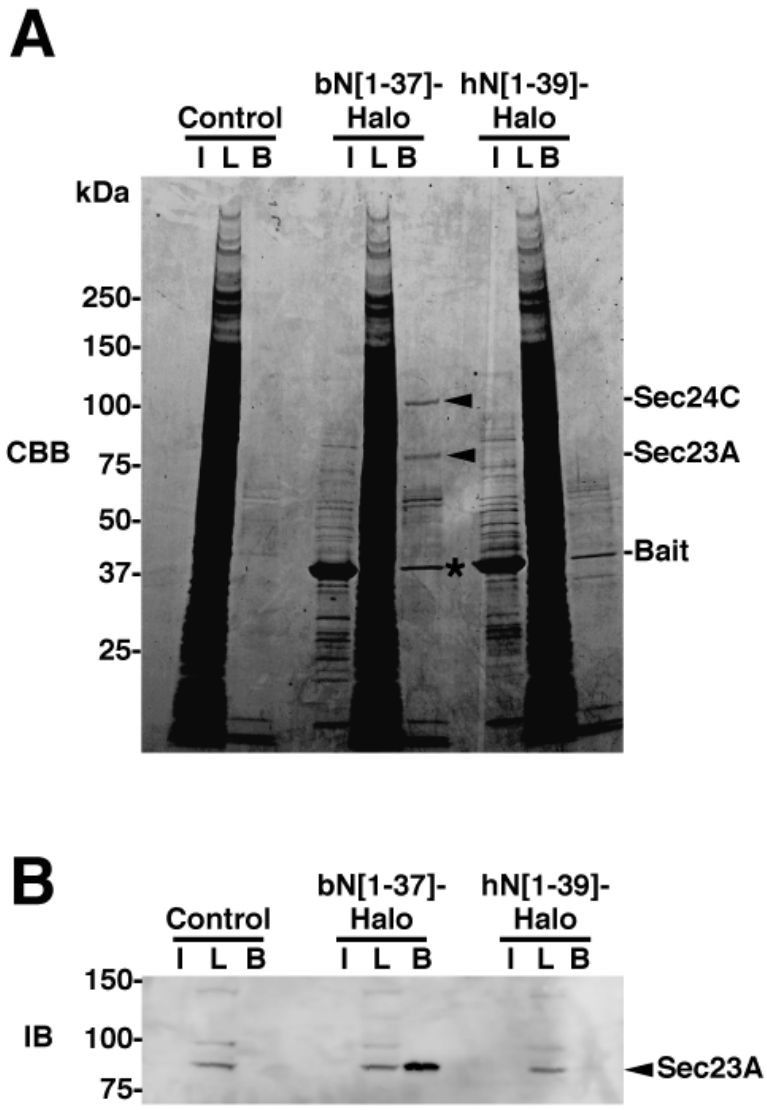

Figure 15. Identification the proteins that specifically interacted with the bN[1–37] sequence. *A*, HEK293 cell lysate (*lane L*) was incubated with bacterially expressed bN[1–37]-Halo or hN[1–39]-Halo protein that was immobilized on HaloLink resin, or with the resin alone (*Control*). Bound proteins (*lane B*) were separated by SDS-PAGE on a 5%–20% gradient gel followed by staining with Coomassie brilliant blue. The 120-kDa and 85-kDa polypeptides that specifically bound to bN[1–37] were subjected to MS/MS analysis and were identified as Sec24C and Sec23A, respectively (indicated by arrowheads). *Lane I* contains the bait protein and the asterisk indicates the bait protein that leaked from the resin. *B*, Immunoblotting with an anti-Sec23A antibody (*IB*) detected a band specifically in the fraction that bound the bN[1–37]-Halo-coupled resin and in the total cell lysate, which migrated at a size comparable with that of the 85-kDa protein shown in *A*. Proteins in each fraction were separated on an 8% gel and were immunoblotted.

Table 2. Summary of MS/MS analysis of the polypeptides that specifically bound to bN[1-37]-Halo

Polypeptides in Fig. 15	Protein identified	IPI accession number	Theoretical molecular mass (kDa)	Number of matched peptides*	Sequence of matched polypeptides†	Sequence coverage (%)§
120 kDa	Protein transport protein Sec24C	IPI00024661.5	118.2	6	SPVESTTEPPAVR	4.38
				1	GTEPFVTGVR	
				3	SDVLQPGAEVTTDDR	
				3	EGGAEESAIR	
85 kDa	Protein transport protein Sec23A	IPI00017375.2	86.1	10	AVLNPLCQVDYR	4.58
				1	AETEEGPDVLR	
				1	GPQVQQPPPSNR	

*Number of tryptic peptides possessing masses matched with those expected for the identified protein.

†The amino acid sequences identified by MS/MS.

§The percentage of amino acid sequences covered by the matched peptides.

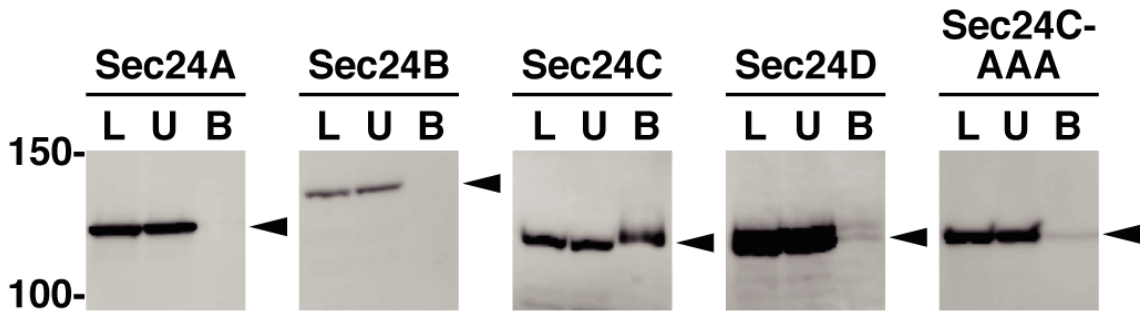

Figure 16. Selective interaction between the bN[1–37] and Sec24C. Lysate from HEK293 cells expressing myc-tagged Sec24 isoforms (*Sec24A*, *Sec24B*, *Sec24C*, *Sec24D*) or Sec24C-AAA, were incubated with bN[1–37]-Halo-coupled resin. Sec24 proteins in cell lysate (*L*), unbound (*U*), and bound (*B*) fractions were detected by immunoblotting with an anti-myc antibody (indicated by arrowheads).

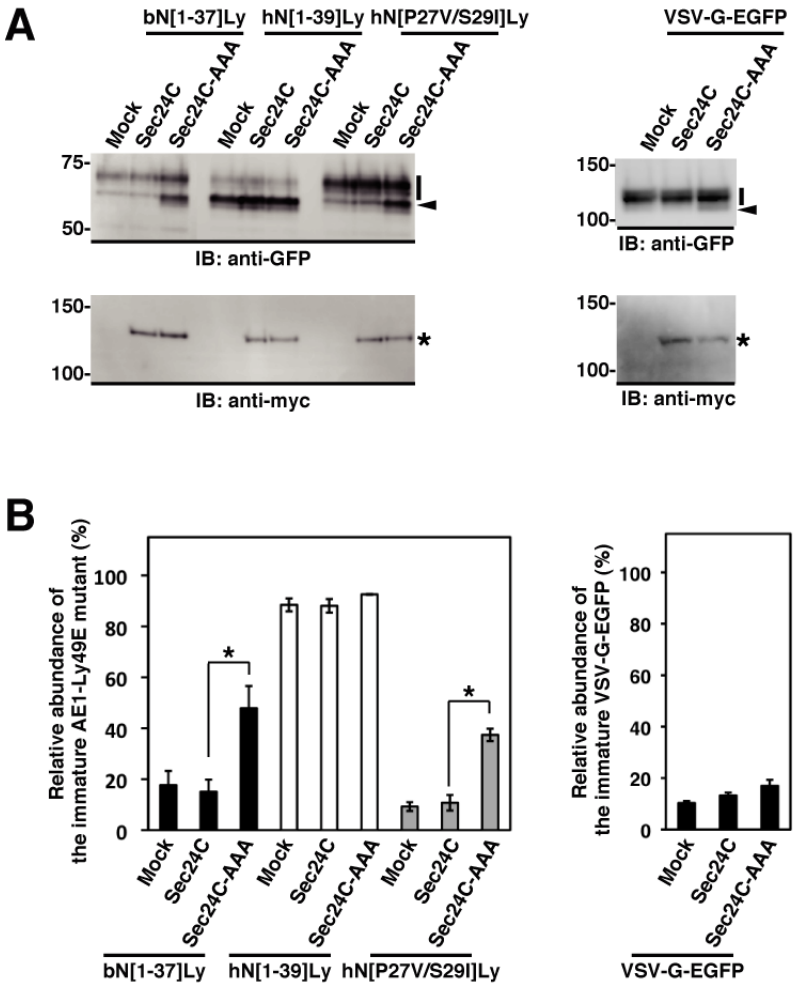

Figure 17. Role of the binding site of Sec24C for the interaction with the ΦXΦXΦ motif. *A*, The effect of Sec24-AAA on *N*-glycan processing of AE1-Ly49E chimeric proteins was examined. HEK293 cells were co-transfected with an AE1-Ly49E mutant (*bN[1–37]Ly*, *hN[1–39]Ly*, or *hN[P27V/S29I]Ly*) or VSV-G-EGFP and either the empty vector (*Mock*), myc-tagged Sec24C (*Sec24C*), or its Sec24C-AAA mutant (*Sec24C-AAA*). After 48 hours, the AE1-Ly49E and VSV-G proteins and Sec24C proteins in the cell lysates were detected by immunoblotting with anti-GFP and anti-myc antibodies, respectively. *Representative* immunoblots from three independent experiments are shown in *A*. The migrating positions of AE1-Ly49E mutants and VSV-G with mature and immature *N*-glycans are indicated by a bar and an arrowhead, respectively. The asterisk indicates Sec24C proteins. The migrating positions of the size markers are shown in kDa. *B*, The abundance of AE1-Ly49E and VSV-G proteins with mature and immature *N*-glycans relative to the total amount were quantitated by densitometric scanning of the immunoblots. Data are expressed as the mean ± S.D. (n = 3, *p<0.05, **p<0.005).

Discussion

The present study identified the ΦXΦXΦ sequence as a new class of sorting signal that facilitates the ER export of cargo proteins through the COPII pathway. Various bovine and human AE1 mutants and Ly49E-based reporter proteins possessing a ΦXΦXΦ motif were targeted to the cell surface with efficient *N*-glycan processing, whereas mutants and reporter proteins lacking this motif were largely retained in the ER (Figs. 2, 4, 5, 7, 8, 10, and 11). The facilitation of ER export by the ΦXΦXΦ motif was also verified by its selective binding to the Sec23A/Sec24C complex (Fig. 15). It is conceivable that the ΦXΦXΦ motif acts as the primary signal for the ER export of cargo proteins, and that a signal in the N-terminus that facilitates the plasma membrane targeting of erythroid AE1 is present in specific species, including cattle, horse, and mouse.

Perhaps the most novel findings of the present study are that the ΦXΦXΦ motif selectively interacts with Sec24C, and that the motif appears to share the binding site on Sec24C with the IXM signal. The Sec24C-AAA mutant, in which the binding site sequence ^{895}LIL^{897} of the IXM motif (Mancias and Goldberg, 2008) was mutated to ^{895}AAA^{897}, no longer interacted with AE1–Ly49E reporter proteins, resulting in their ER retention (Fig. 17). The ΦXΦXΦ motif sequence ^{26}VSIPM^{30} in bovine AE1 includes ^{28}IPM^{30}, which is comparable with the IXM class ER export signal of membrin and syntaxin 5 (Mancias and Goldberg, 2008). Conversely, the IXM motif and the sequence upstream of this motif in mammalian syntaxin 5 consists of VXIXM (^{189}VAIDM^{193} in the human sequence), which is comparable

with the ΦXΦXΦ sequence. However, these two motifs differ from each other in the following respects. Firstly, while the IXM motif binds in the surface groove of Sec24C and Sec24D (Mancias and Goldberg, 2008), the ΦXΦXΦ motif specifically binds to Sec24C but not to Sec24D (Fig. 16). Secondly, creation of the ^{29}IQM^{31} sequence in hAE1Δ11 (hAE1Δ11/S29I) resulted in ER retention of the protein, and the coordinate mutation of Pro^{27} to generate the ^{27}VEIQM^{31} sequence (hAE1Δ11/P27V/S29I) was needed for efficient *N*-glycan processing and cell surface expression (Fig. 8). Therefore, the selective interaction between the ΦXΦXΦ motif and Sec24 is likely due to structural differences between Sec24C and Sec24D in the region adjacent to the binding site with the LIL sequence, as well as to the structure of the motif on the cargo. Sec24C or Sec24D are absolutely required for binding the RI/RL motif of the highly related SLC6 family transporters (Farhan *et al*., 2007; Sucic *et al*., 2011). The serotonin transporter, SERT, and the GABA transporter, GAT1, interact with Sec24C and Sec24D, respectively, although both transporters bind to the relevant DD sequence on Sec24C/Sec24D machineries (Farhan *et al*., 2007; Sucic *et al*., 2011).

As demonstrated by the previous structural analyses of the cytoplasmic domain of human erythroid AE1, a large part of the N-terminal stretch (the first 54 residues in human AE1 corresponding to residues 1–64 in bovine AE1 containing the ^{26}VSIPM^{30} sequence) is flexible and dynamically disordered (Zhang *et al*., 2000; Zhou *et al*., 2005). When AE1 forms tetramers in the membrane, two of the N-terminal regions on the distal monomers in the tetramer, which are not involved in the association with the bridging protein ankyrin, are anticipated to be in close proximity to the lipid bilayer (Zhang *et al*., 2000). On the other hand,

the common binding pocket for the ΦXΦXΦ and IXM motifs containing the ^{895}LIL^{897} sequence in the distal region of Sec24C in the Sec23/Sec24-Sar1 complex faces towards, and is close proximity to, the membrane (Bi *et al*., 2002; Mancias and Goldberg, 2005; Mancias and Goldberg, 2008). Therefore, it is likely that the interaction of the AE1 ΦXΦXΦ motif with Sec24C readily occurs on the surface close to the ER membrane. AE1 exists primarily as a mixture of dimers and tetramers in membranes (Van Dort *et al*., 1998) and AE1 forms a dimer in the ER (Ito *et al*., 2006). Binding of ankyrin induces two dimers to form a tetramer (Michaely and Bennett, 1995; Van Dort *et al*., 1998) and this AE1-ankyrin interaction occurs in the ER when both proteins are exogenously expressed (Gomez and Morgans, 1993; Adachi *et al*., 2010). These findings indicate that AE1 is present as a dimer and forms a tetramer in the ER when ankyrin is available. Hence, the interaction between the ΦXΦXΦ motif and Sec24C may contribute to cooperative incorporation and concentration of AE1, ankyrin, and the COPII machineries into pre-budding vesicles.

Our observations on the N-terminal ER export signal do not rule out the possibility that an unidentified signal(s) also participates in the plasma membrane targeting of AE1. Indeed human and canine AE1, which do not have a ΦXΦXΦ motif in the N-terminus, are transported to the plasma membrane in red blood cells. In fact, cell surface biotinylation and *N*-glycan maturation of AE1 mutants and AE1–Ly49E mutants lacking this motif (*e.g*. hAE1Δ11 and hN[1–39]Ly *etc*., Figs. 2, 8, and 10) were detected, although at with much lower efficiency than those of proteins bearing the ΦXΦXΦ motif. A marked fraction of hN[1–39]Ly containing the first 39 residues of human AE1 exited the ER (Fig. 11) and this

region has no known ER export signal, except for several di-acidic sequences representing the (D/E)X(D/E) motif; therefore, any of these di-acidic residues are candidate ER exit signals for erythroid AE1 in various species including humans (Fig. 1). The highly conserved ELXXL(D/E) (^{882}ELQCLD^{887} in human AE1) in the C-terminal region is another candidate signal. This sequence is essential for the proper targeting of erythroid AE1 to the cell surface in HEK293 cells (Adachi *et al*., 2009) and matches the LXXLE class of ER export signal found in the yeast SNARE protein Bet1 (Miller *et al*., 2003; Mossessova *et al*., 2003). Di-acidic and LXXLE motifs share the same binding site on mammalian Sec24A and Sec24B (Mancias and Goldberg, 2008; Russell and Stagg, 2010; Zanetti *et al*., 2012).

We do not have a rational explanation for why the sequences of ER export signals of AE1 exhibit such variability in mammals. However, such sequence variability might occur in many proteins, and different signal motifs might be used in different contexts or be part of a compensatory mechanism for the intracellular trafficking of a single protein species. For example, we are intrigued by the possible use of distinct signal motifs in different mammals for the interaction between neutrophil lysosomal elastase and the AP-3 adaptor protein complex. Mutations in the AP3B1 gene, which encodes the β subunit of AP-3, are responsible for cyclic neutropenia, which is associated with a deficiency of neutrophil elastase (ELA2), in humans and dogs (Benson *et al*., 2003). However, the tyrosine-based signal in human ELA2, which interacts with AP-3 (Benson *et al*., 2003), is not conserved in canine ELA2 (GenBank accession number, AF494190). This suggests that a different signal motif, such as a di-leucine signal that is recognized by AP-3 (Horwitz *et al*., 2004), is used to target ELA2 to lysosomes

in dogs. Moreover, clathrin-mediated endocytosis of bovine AE1 uses a non-canonical YXXXΦ motif instead of the YXXΦ signal (Wang *et al*., 2012), and this is another example of variability in the sequences of motifs used for cargo recognition.

In conclusion, we demonstrate that a novel ΦXΦXΦ sequence functions as an ER export signal through selective binding to the pre-budding complex component Sec24C. Elucidation of the mechanism responsible for the ΦXΦXΦ motif-Sec24C interaction and the cargo molecules that utilize this interaction to exit the ER may shed further light on the mechanisms underlying intracellular trafficking of membrane and secretory proteins, and on the etiology of diseases that are caused by impaired trafficking.

References

Adachi, H., Ito, D., Kurooka, T., Otsuka, Y., Arashiki, N., Sato, K., and Inaba, M. (2009) Structural implications of the EL(KIQ)(L/C)LD(A/G)DD sequence in the C-terminal cytoplasmic tail for proper targeting of anion exchanger 1 to the plasma membrane. *Jpn. J. Vet. Res.* **57**, 135-146.

Adachi, H., Kurooka, T., Otsu, W., and Inaba, M. (2010) The forced aggresome formation of a bovine anion exchanger 1 (AE1) mutant through association with deltaF508-cystic fibrosis transmembrane conductance regulator upon proteasome inhibition in HEK293 cells. *Jpn. J. Vet. Res.* **58**, 101-110.

Alper, S. L. (2006) Molecular physiology of SLC4 anion exchangers. *Exp. Physiol.* **91**, 153-161.

Aridor, M., Bannykh, S. I., Rowe, T., and Balch, W. E. (1995) Sequential coupling between COPII and COPI vesicle coats in endoplasmic reticulum to Golgi transport. *J. Cell Biol.* **131**, 875-893.

Benson, K. F., Li, F. Q., Person, R. E., Albani, D., Duan, Z., Wechsler, J., Meade-White, K., Williams, K., Acland, G. M., Niemeyer, G. Lothrop, C. D., and Horwitz, M. (2003) Mutations associated with neutropenia in dogs and humans disrupt intracellular transport of neutrophil elastase. *Nat. Genet.* **35**, 90-96.

Bi, X., Corpina, R. A., and Goldberg, J. (2002) Structure of the Sec23/24-Sar1 pre-budding complex of the COPII vesicle coat. *Nature* **419**, 271-277.

Bonifacino, J. S. and Glick, B. S. (2004) The mechanisms of vesicle budding and fusion. *Cell* **116**, 153-166.

Devonald, M. A., Smith, A. N., Poon, J. P., Ihrke, G., and Karet, F. E. (2003) Non-polarized targeting of AE1 causes autosomal dominant distal renal tubular acidosis. *Nat. Genet.* **33**, 125-127.

Farhan, H., Reiterer, V., Korkhov, V. M., Schmid, J. A., Freissmuth, M., and Sitte, H. H. (2007) Concentrative export from the endoplasmic reticulum of the gamma-aminobutyric acid transporter 1 requires binding to SEC24D. *J. Biol. Chem.* **282**, 7679-7689.

Gillon, A. D., Latham, C. F., and Miller, E. A. (2012) Vesicle-mediated ER export of proteins and lipids. *Biochim. Biophys. Acta* **1821**, 1040-1049.

Gomez, S. and Morgans, C. (1993) Interaction between band 3 and ankyrin begins in early compartments of the secretory pathway and is essential for band 3 processing. *J. Biol. Chem.* **268**, 19593-19597.

Horwitz, M., Benson, K. F., Duan, Z., Li, F. Q., and Person, R. E. (2004) Hereditary neutropenia, dogs explain human neutrophil elastase mutations. *Trends Mol. Med.* **10**, 163-170.

Inaba, M., Yawata, A., Koshino, I., Sato, K., Takeuchi, M., Takakuwa, Y., Manno, S., Yawata, Y., Kanzaki, A., Sakai, J., Ban, A., Ono, K., and Maede, Y. (1996) Defective anion transport and marked spherocytosis with membrane instability caused by hereditary total deficiency of red cell band 3 in cattle due to a nonsense mutation. *J. Clin. Invest.* **97**, 1804-1817.

Ito, D., Koshino, I., Arashiki, N., Adachi, H., Tomihari, M., Tamahara, S., Kurogi, K., Amano, T., Ono, K., and Inaba, M. (2006) Ubiquitylation-independent ER-associated degradation of an AE1 mutant associated with dominant hereditary spherocytosis in cattle. *J. Cell Sci.* **119**, 3602-3612.

Khoriaty, R., Vasievich, M. P., and Ginsburg, D. (2012) The COPII pathway and hematologic disease. *Blood* **120**, 31-38.

Ma, D., Zerangue, N., Lin, Y. F., Collins, A., Yu, M., Jan, Y. N., and Jan, L. Y. (2001) Role of ER export signals in controlling surface potassium channel numbers. *Science* **291**, 316-319.

Mancias, J. D. and Goldberg, J. (2005) Exiting the endoplasmic reticulum. *Traffic* **6**, 278-285.

Mancias, J. D. and Goldberg, J. (2008) Structural basis of cargo membrane protein discrimination by the human COPII coat machinery. *EMBO J*. **27**, 2918-2928.

Mellman, I. and Nelson, W. J. (2008) Coordinated protein sorting, targeting and distribution in polarized cells. *Nat. Rev. Mol. Cell Biol*. **9**, 833-845.

Michaely, P. and Bennett, V. (1995) The ANK repeats of erythrocyte ankyrin form two distinct but cooperative binding sites for the erythrocyte anion exchanger. *J. Biol. Chem*. **270**, 22050-22057.

Miller, E. A., Beilharz, T. H., Malkus, P. N., Lee, M. C., Hamamoto, S., Orci, L., and Schekman, R. (2003) Multiple cargo binding sites on the COPII subunit Sec24p ensure capture of diverse membrane proteins into transport vesicles. *Cell* **114**, 497-509.

Mossessova, E., Bickford, L. C., and Goldberg, J. (2003) SNARE selectivity of the COPII coat. *Cell* **114**, 483-495.

Nishimura, N. and Balch, W. E. (1997) A di-acidic signal required for selective export from the endoplasmic reticulum. *Science* **277**, 556-558.

Nufer, O., Guldbrandsen, S., Degen, M., Kappeler, F., Paccaud, J. P., Tani, K., and Hauri, H. P. (2002) Role of cytoplasmic C-terminal amino acids of membrane proteins in ER export. *J. Cell Sci*. **115**, 619-628.

Nufer, O., Kappeler, F., Guldbrandsen, S., and Hauri, H. P. (2003) ER export of ERGIC-53 is controlled by cooperation of targeting determinants in all three of its domains. *J. Cell Sci*. **116**, 4429-4440.

Okkenhaug, H., Weylandt, K. H., Carmena, D., Wells, D. J., Higgins, C. F., and Sardini, A. (2006) The human ClC-4 protein, a member of the CLC chloride channel/transporter family, is localized to the endoplasmic reticulum by its N-terminus. *FASEB J*. **20**, 2390-2392.

Quilty, J. A., Cordat, E., and Reithmeier, R. A. (2002) Impaired trafficking of human kidney

anion exchanger (kAE1) caused by hetero-oligomer formation with a truncated mutant associated with distal renal tubular acidosis. *Biochem. J.* **368**, 895-903.

Russell, C. and Stagg, S. M. (2010) New insights into the structural mechanisms of the COPII coat. *Traffic* **11**, 303-310.

Sucic, S., El-Kasaby, A., Kudlacek, O., Sarker, S., Sitte, H. H., Marin, P., and Freissmuth, M. (2011) The serotonin transporter is an exclusive client of the coat protein complex II (COPII) component SEC24C. *J. Biol. Chem.* **286**, 16482-16490.

Tanner, M. J. (2002) Band 3 anion exchanger and its involvement in erythrocyte and kidney disorders. *Curr. Opin. Hematol.* **9**, 133-139.

Toye, A. M., Bruce, L. J., Unwin, R. J., Wrong, O., and Tanner, M. J. (2002) Band 3 Walton, a C-terminal deletion associated with distal renal tubular acidosis, is expressed in the red cell membrane but retained internally in kidney cells. *Blood* **99**, 342-347.

Toye, A. M., Banting, G., and Tanner, M. J. (2004) Regions of human kidney anion exchanger 1 (kAE1) required for basolateral targeting of kAE1 in polarised kidney cells, mis-targeting explains dominant renal tubular acidosis (dRTA). *J. Cell Sci.* **117**, 1399-1410.

Tzetis, M., Efthymiadou, A., Strofalis, S., Psychou, P., Dimakou, A., Pouliou, E., Doudounakis, S., and Kanavakis, E. (2001) CFTR gene mutations--including three novel nucleotide substitutions--and haplotype background in patients with asthma, disseminated bronchiectasis and chronic obstructive pulmonary disease. *Hum. Genet.* **108**, 216-221.

Van Beneden, K., Stevenaert, F., De Creus, A., Debacker, V., De Boever, J., Plum, J., and Leclercq, G. (2001) Expression of Ly49E and CD94/NKG2 on fetal and adult NK cells. *J. Immunol.* **166**, 4302-4311.

Van Dort, H. M., Moriyama, R., and Low, P. S. (1998) Effect of band 3 subunit equilibrium on the kinetics and affinity of ankyrin binding to erythrocyte membrane vesicles. *J. Biol. Chem.* **273**, 14819-14826.

Wang, C. C., Sato, K., Otsuka, Y., Otsu, W., and Inaba, M. (2012) Clathrin-mediated endocytosis of mammalian erythroid AE1 anion exchanger facilitated by a YXXPhi or a noncanonical YXXXPhi motif in the N-terminal stretch. *J. Vet. Med. Sci.* **74**, 17-25.

Wang, X., Matteson, J., An, Y., Moyer, B., Yoo, J. S., Bannykh, S., Wilson, I. A., Riordan, J. R., and Balch, W. E. (2004) COPII-dependent export of cystic fibrosis transmembrane conductance regulator from the ER uses a di-acidic exit code. *J. Cell Biol.* **167**, 65-74.

Wendeler, M. W., Paccaud, J. P., and Hauri, H. P. (2007) Role of Sec24 isoforms in selective export of membrane proteins from the endoplasmic reticulum. *EMBO Rep.* **8**, 258-264.

Williamson, R. C., Brown, A. C., Mawby, W. J., and Toye, A. M. (2008) Human kidney anion exchanger 1 localisation in MDCK cells is controlled by the phosphorylation status of two critical tyrosines. *J. Cell Sci.* **121**, 3422-3432.

Yenchitsomanus, P. T., Kittanakom, S., Rungroj, N., Cordat, E., and Reithmeier, R. A. (2005) Molecular mechanisms of autosomal dominant and recessive distal renal tubular acidosis caused by SLC4A1 (AE1) mutations. *J. Mol. Genet. Med.* **1**, 49-62.

Yokoyama, W. M. and Plougastel, B. F. (2003) Immune functions encoded by the natural killer gene complex. *Nat. Rev. Immunol.* **3**, 304-316.

Zanetti, G., Pahuja, K. B., Studer, S., Shim, S., and Schekman, R. (2012) COPII and the regulation of protein sorting in mammals. *Nat. Cell Biol.* **14**, 20-28.

Zhang, D., Kiyatkin, A., Bolin, J. T., and Low, P. S. (2000) Crystallographic structure and functional interpretation of the cytoplasmic domain of erythrocyte membrane band 3. *Blood* **96**, 2925-2933.

Zhou, Z., DeSensi, S. C., Stein, R. A., Brandon, S., Dixit, M., McArdle, E. J., Warren, E. M., Kroh, H. K., Song, L., Cobb, C. E., Hustdt, E. J., and Beth, A. H. (2005) Solution structure of the cytoplasmic domain of erythrocyte membrane band 3 determined by

site-directed spin labeling. *Biochemistry* **44**, 15115-15128.

Zhu, Q., Lee, D. W., and Casey, J. R. (2003) Novel topology in C-terminal region of the human plasma membrane anion exchanger, AE1. *J. Biol. Chem.* **278**, 3112-3120.

Acknowledgements

The author expresses sincere gratitude to Professor Mutsumi Inaba (Laboratory of Molecular Medicine, Graduate School of Veterinary Medicine, Hokkaido University) for his excellent supervision and encouragements throughout this work.

I would like to express my great thanks to Professor Kazuhiro Kimura (Laboratory of Biochemistry), Associate Professor Tohru Yamamori (Laboratory of Radiation Biology), and Associate Professor Kota Sato (Laboratory of Molecular Medicine), all from Graduate School of Veterinary Medicine, Hokkaido University, for their helpful discussion and critical reading of the manuscript. I also express my great thanks to Dr. Takao Kurooka (Safety Research Laboratory, R & D, Kissei Pharmaceutical Co. Ltd.), Dr. Yayoi Otsuka (Laboratory of Molecular Medicine) and all members of the Laboratory of Molecular Medicine for their helpful discussions and technical assistances.

Abstract

Protein export from the endoplasmic reticulum (ER) depends on the interaction between a signal motif on the cargo and a cargo-recognition site on the coatomer protein complex II (COPII). A hydrophobic sequence in the N-terminus of the bovine AE1 anion exchanger facilitated the ER export of human AE1Δ11, an ER-retained AE1 mutant, through interaction with a specific Sec24 isoform. The cell surface expression and *N*-glycan processing of various substitution mutants or chimeras of human and bovine AE1 proteins and their Δ11 mutants in HEK293 cells were examined. The N-terminal sequence (V/L/F)X(I/L)X(M/L), ^{26}VSIPM^{30} in bovine AE1, which is comparable with ΦXΦXΦ, acted as the ER export signal for AE1 and AE1Δ11 (Φ is a hydrophobic amino acid and X is any amino acid). The AE1-Ly49E chimeric protein possessing the ΦXΦXΦ motif exhibited effective cell surface expression and *N*-glycan maturation via the COPII pathway, whereas a chimera lacking this motif was retained in the ER. A synthetic polypeptide containing the N-terminus of bovine AE1 bound the Sec23A/Sec24C complex through a selective interaction with Sec24C. Co-transfection of Sec24C-AAA, in which the residues ^{895}LIL^{897} (the binding site for another ER export signal motif IXM on Sec24C and Sec24D) were mutated to ^{895}AAA^{897} specifically increased ER retention of the AE1-Ly49E chimera. These findings demonstrate that the ΦXΦXΦ sequence functions as a novel signal motif for the ER export of cargo proteins through an exclusive interaction with Sec24C.

Abstract in Japanese (要　旨)

学位論文題名

A New Class of Endoplasmic Reticulum Export Signal ΦXΦXΦ for Transmembrane Proteins and its Selective Interaction with Sec24C

（膜蛋白質小胞体輸出の分子機構：新規シグナル配列ΦXΦXΦと Sec24C の選択的相互作用）

小胞体(ER)で合成された膜内在性蛋白質は、Sar1-GTP と Sec23/Sec24、Sec13/Sec31 各複合体から構成される coatomer protein complex II (COPII)小胞に組み込まれてゴルジ装置へ運ばれる。この小胞輸出には、積荷蛋白質の特定アミノ酸配列モチーフ(ER 輸出シグナル)が Sec24 と選択的に結合することが必要である。Di-acidic 配列、di-hydrophobic 配列をはじめとする多様な ER 輸出シグナルと Sec24 分子の多様性が、多くの蛋白質の COPII 小胞への組み込みを可能としているとされるが、具体的な相互作用が明らかにされている例は少ない。

AE1 (anion exchanger 1、バンド 3)は、赤血球と腎臓集合管上皮細胞に分布する膜内在性蛋白質である。AE1 遺伝子の異常に起因する遺伝性球状赤血球症や遠位尿細管アシドーシスの分子病態解析から、ヒト AE1 の極性分布や非極性細胞における細胞膜への輸送には C 末端 11 アミノ酸残基が必須であることが明らかにされている。例えば、HEK293 細胞に発現させた C 末端 11 アミノ酸を欠く変異体(AE1Δ11)は、細胞膜に輸送されず ER に滞留する。ところが、牛の AE1 を HEK293 細胞に導入すると、牛 AE1Δ11 は野生型と同様の効率で細胞膜に運ばれ、ER への滞留はみられない。したがって、その ER からの輸出は、ヒトとは異なる未知のシグナルで規定されることが示唆される。本研究の目的は、AE1 の ER 輸出に関わる新たなシグナルを同定し、そのメカニズムを解明することにある。

まず、AE1 と AE1Δ11 の N 末端細胞質ドメインに焦点をあて、一連の牛–ヒトキメラ蛋白質を作製し HEK293 細胞に発現させてそれらの細胞内局在を比較した。AE1 蛋白質は N 末端に enhanced green fluorescent protein (EGFP)を付加して細胞内分布を観察し、また細胞表面ビオチン化法で細胞膜における発現を解析した。その結果、N 末端領域の ^{25}SVSIPM^{30} 配列が牛 AE1 の細胞膜における発現を規定することが判明した。この配列のアミノ酸置換変異体について同様の解析を行った結果、^{26}VSIPM^{30} 部分が(V/L/F)X(I/L)X(M/L)である場合に EGFP-AE1、EGFP-AE1Δ11 はいずれも細胞表面に効率よく輸送される一方、いずれかの疎水性アミノ酸のアラニン置換体は全て ER への滞留を示した。したがって、このΦXΦXΦ配列(Φ は疎水性、X は任意のアミノ酸残基)が、ER からの小胞輸出を規定するシグナルとなる可能性が示された。

次に、II 型膜貫通性蛋白質である Ly49E の N 末端細胞質領域を AE1 のそれと組み換えた

EGFP 標識キメラレポーター蛋白質の細胞内局在を、上記の手法に糖鎖成熟の解析を加えて検討した。ΦXΦXΦ配列を持たないヒト AE1 の N 末端領域を組み込んだ hN[1-39]Ly の蛍光シグナルの大部分が ER に分布したのとは対照的に、牛 AE1 由来の ^{26}VSIPM^{30}配列をもつ bN[1-37]Ly とヒト AE1 N 末端領域にΦXΦXΦ配列を持たせた hN[P27V/S29I]Ly のシグナルは主に細胞膜に認められた。また、hN[1-39]Ly の *N*-結合型糖鎖が endoglycosidase H に感受性の高マンノース型でありゴルジ装置における糖鎖成熟が生じていないのに対し、bN[1-37]Ly と hN[P27V/S29I]Ly は同酵素に耐性であった。さらに、Sar1 H79G 変異体を同時に発現させて COPII 小胞の形成を阻害したところ、bN[1-37]Ly と hN[P27V/S29I]Ly の *N*-結合型糖鎖の成熟が阻害された。加えて、牛 AE1 と同様、ΦXΦXΦに相当する配列をもつ馬(^{11}IEVIV^{15})とマウス(^{35}LTIPV^{39})の AE1Δ11、ならびにその N 末端領域と Ly49E のキメラ蛋白質(それぞれ eqN[1-41]Ly と mN[1-49]Ly)は、導入した HEK293 細胞で、いずれも細胞膜における発現を呈したが、相当する配列のない犬 AE1Δ11 とキメラ蛋白質 cN[1-46]Ly は ER への滞留を生じた。これらの結果から、ΦXΦXΦ配列は、レポーター蛋白質の COPII 小胞による ER からの輸出シグナルとして働くことが明らかになった。

最後に、このΦXΦXΦ配列の COPII 小胞側の受け手となる分子の検討を行った。牛 AE1 の N 末端領域に Halo tag を付加したリコンビナントペプチド bN[1-37]-Halo を作製し、同じくヒト配列由来の hN[1-39]-Halo を対照として、HEK293 細胞の可溶化抽出蛋白質と孵置し、特異的に結合する蛋白質を得た。これらの蛋白質をトリプシン消化のうえ質量分析装置で解析したところ、Sec24C と Sec23A であることが示唆された。そこで、Sec24A〜Sec24D を発現させた HEK293 細胞抽出液と上記のリコンビナントペプチドを孵置したところ、Sec24C が bN[1-37]-Halo と特異的に結合することが判明した。さらに、Sec24C/Sec24D 上の IXM モチーフ結合部位として知られる ^{895}LIL^{897} をアラニンに置換した Sec24C-AAA 変異体では、リコンビナントペプチドとの結合が失われ、またこれを同時に細胞に導入すると、bN[1-37]Ly と hN[P27V/S29I]Ly の糖鎖成熟が阻害された。これらの結果は、Sec24C がΦXΦXΦ配列を特異的に認識・結合する COPII 小胞側の受け手として機能し、その結合が ^{895}LIL^{897} を含む領域で生じることを明示している。

以上の知見から、新たなモチーフ配列ΦXΦXΦが膜内在性蛋白質の ER 輸出シグナルとして働くこと、このΦXΦXΦシグナルは Sec24C との特異的結合を介して積荷蛋白質の COPII 小胞への組み込みと ER–ゴルジ間小胞輸送を効率化することが解明された。